

*Digital Comprehensive Summaries of Uppsala Dissertations
from the Faculty of Science and Technology 2424*

Single-cell oxygen metabolism: a universal, effect-based marker of chemical toxicity

YUAN CUI



ACTA UNIVERSITATIS
UPSALIENSIS
2024

ISSN 1651-6214
ISBN 978-91-513-2182-0
urn:nbn:se:uu:diva-535367



UPPSALA
UNIVERSITET

Dissertation presented at Uppsala University to be publicly examined in Ekmensalen, EBC, Norbyvägen 16, Uppsala, Friday, 13 September 2024 at 09:15 for the degree of Doctor of Philosophy. The examination will be conducted in English. Faculty examiner: Professor Nicole Pamme (Stockholm University).

Abstract

Cui, Y. 2024. Single-cell oxygen metabolism: a universal, effect-based marker of chemical toxicity. *Digital Comprehensive Summaries of Uppsala Dissertations from the Faculty of Science and Technology* 2424. 64 pp. Uppsala: Acta Universitatis Upsaliensis. ISBN 978-91-513-2182-0.

Understanding how organisms respond to oxygen (O₂) fluctuations in their aquatic microenvironments and studying O₂ consumption as an indicator of metabolism is crucial for advancing ecology, toxicology, tissue engineering and environmental sciences. However, despite their importance across scientific disciplines, traditional O₂ measurements often lack the sensitivity to capture rapid or localized changes occurring at the microscale. This PhD thesis addresses this challenge by developing novel microfluidic techniques and systems to sense O₂.

To investigate advective and diffusive O₂ fluxes at the microscale, this thesis developed chemical sensing particle image velocimetry (sensPIV), a technique that combines optode microparticles and rapid microscope imaging. Specifically, I contributed by testing the performance of sensPIV particles within O₂-permeable polydimethylsiloxane (PDMS) devices. This demonstrated the effectiveness of sensPIV in visualizing microscale O₂ fluxes, with potential applications around complex biological structures such as coral segments.

To characterize single-cell O₂ respiration rates this thesis developed a micro-respiration chamber device. This device consists of gastight microwells that isolate single-cells, allowing for measuring their O₂ consumption via immobilized O₂-sensitive optodes. When applied to human hepatic cells, this device revealed size-related respiration kinetics in single-cells and adaptively changing respiration rates due to O₂ limitations. The micro-respiration device was then refined into SlipO₂Chip, a microfluidic platform that quantifies single-cell O₂ respiration rates before and after chemical exposures. This was achieved by adding a mechanism for opening and closing microwells via slipping a dedicated channel that introduces chemical solutions. SlipO₂Chip demonstrated a dose-dependent decrease in diatom respiration when exposed to the bacterial infochemical 2-Heptyl-4-Quinolone (HHQ), thus enhancing our understanding of toxicological impacts by detailing cell-to-cell heterogeneity. In a final effort, the micro-respiration chamber device was combined with quantitative phase imaging (QPI) to jointly measure respiration rates and dry mass in individual cells from three unicellular diatom species of varying sizes (16 - 300 µm). Preliminary data were integrated into metabolic scaling theory that describes how metabolic rates scale with geometrical size/mass across all species. The results indicated an interspecific scaling exponent similar to published bulk measures, and three intraspecific exponents showing potential morphological and physiological relationships to metabolism. This proof-of-concept study highlighted that combined measurement of metabolism and mass can enhance the resolution of scaling theory by adding crucial information on cell-to-cell variability.

Overall, this PhD thesis contributed to ecotoxicology, ecology and bioengineering by providing detailed insights into spatiotemporal O₂ dynamics and single-cell O₂ metabolism in the presence and absence of chemical perturbations.

Keywords: O₂ metabolism, Intracellular respiration, Single-cell analysis, Mass flux, Optodes, Micro-chamber, Microwell, Phytoplankton, Diatom, Human hepatic cell, 2-Heptyl-4-Quinolone (HHQ), Dose-response relationship, Dry mass, Quantitative phase imaging (QPI), Metabolic scaling theory, Toxicology, Microfluidics, Lab on a chip

Yuan Cui, Department of Organismal Biology, Physiology and Environmental Toxicology, Norbyvägen 18 A-D, Uppsala University, SE-752 36 Uppsala, Sweden.

© Yuan Cui 2024

ISSN 1651-6214

ISBN 978-91-513-2182-0

URN urn:nbn:se:uu:diva-535367 (<http://urn.kb.se/resolve?urn=urn:nbn:se:uu:diva-535367>)

To my parents



List of Papers

This thesis is based on the following papers, which are referred to in the text by their Roman numerals.

- I. Ahmerkamp, S.*, Jalaluddin, F. M.*, **Cui, Y.***, Brumley, D. R., Pacherras, C. O., Berg, J. S., Stocker, R., Kuypers, M. M.M., Koren, K., Behrendt, L. (2022) Simultaneous visualization of flow fields and O₂ concentrations to unravel transport and metabolic processes in biological systems. *Cell Reports Methods*, 2(5)
- II. Botte, E.*, **Cui, Y.***, Magliaro, C., Tenje, M., Koren, K., Rinaldo, A., Stocker, R., Behrendt, L., Ahluwalia, A. (2024) Size-related variability of oxygen consumption rates in individual human hepatic cells. *Lab-on-a-Chip*
- III. **Cui, Y.**, Moreira, M. D. A., Whalen, K. E., Barbe, L., Shi, Q., Koren, K., Tenje, M., Behrendt, L. (2024) SlipO₂Chip- single-cell respiration under tuneable environments. Manuscript. In review, *Lab-on-a-Chip*
- IV. **Cui, Y.**, Koren, K., Tenje, M., Behrendt, L. (2024) Combined measurement of oxygen respiration and dry mass on diatom single-cells. Manuscript. In preparation.

* *Shared first authorship, contributed equally to the manuscript.*

Reprints were made with permission from publishers.

Author's contributions

- I. Majority of device design, fabrication, experimental work, analysis, model validation, and writing related to microfluidic parts.
- II. Device design, fabrication, majority of experimental measurement, part of data processing, and writing related to microfluidic parts.
- III. Most part of device designing, fabrication, experiment, analysis and writing.
- IV. Most part of device designing, fabrication, experiment, analysis and writing.

Other contributions

Article not included in this thesis:

- I. Pontén, O., Xiao, L., Kutter, J., **Cui, Y.**, Wählby, C., Behrendt, L. (2024) PACMan: A software package for automated single-cell chlorophyll fluorometry. *Cytometry Part A*, 105(3):203-213

Relevant peer-reviewed work presented at conferences:

- I. **Cui, Y.**, Botte, E., Moreira, M. D. A., Tenje, M., Magliaro, C., Ahluwalia, A., Behrendt, L. (2022) A novel microfluidic device for measuring single-cell oxygen metabolism. Swedish Microfluidics in Life Science (SMILS), poster presentation
- II. **Cui, Y.**, Botte, E., Ahluwalia, A., Tenje, M., Koren, K., Behrendt, L. (2023) Combined measurements of single-cell oxygen metabolism and dry mass. ASLO Aquatic Sciences Meeting, oral presentation

Contents

Introduction and Research Aim	13
Chapter 1: Microscale O ₂ Fluxes and Cellular O ₂ Metabolic: Insights into Bioprocesses	17
O ₂ fluxes in microenvironments	17
O ₂ metabolism in toxicological studies	18
Chapter 2: O ₂ Measurement at the Microscale	22
Microfluidics: an overview	22
Materials and fabrications of microfluidic devices	23
Lab-on-a-Chip: integration of microfluidics with O ₂ measurements	27
Verification.....	34
Chapter 3: Applications of Microscale O ₂ Measurements and Findings	36
SensPIV: tracking O ₂ fluxes at the microscale.....	36
Micro-respiration chamber: size-related respiration kinetics of single hepatic cells	37
SlipO ₂ Chip: O ₂ metabolic changes of diatom single-cells under HHQ treatments.....	38
Combining micro-respiration chamber with QPI: incorporating bio-variability into metabolic scaling theory.....	39
Chapter 4: Concluding Remarks and Future Perspectives	41
Chapter 5: Summary of the Included Papers	43
Paper I: Simultaneous visualization of flow fields and O ₂ concentrations to unravel transport and metabolic processes in biological systems	43
Paper II: Size-related variability of O ₂ consumption rates in individual human hepatic cells.....	44
Paper III: SlipO ₂ Chip- single-cell respiration under tuneable environments	45
Paper IV: Combined measurements of single-cell oxygen metabolism and dry mass	46
Popular Science Summary	47
Populärvetenskaplig sammanfattning	50
Acknowledgements.....	53
Bibliography	55

Abbreviations

CO ₂	Carbon Dioxide
O ₂	Oxygen
HED	Human Equivalent Dose
QPI	Quantitative Phase Imaging
HHQ	2-Heptyl-4-Quinolone
sensPIV	Chemical Sensing Particle Image Velocimetry
ATP	Adenosine Triphosphate
ETC	Electron Transport Chain
HIF-1	Hypoxia-Inducible Factor-1
ROS	Reactive Oxygen Species
OCR	Oxygen Consumption Rate
QS	Quorum Sensing
PDMS	Polydimethylsiloxane
N ₂	Nitrogen Gas
CA	Compressed Air
PtTFPP	Pt(II) meso-Tetra(pentafluorophenyl)porphine
RIE	Reactive Ion Etching Machine
Al	Aluminum
HF	Hydrofluoric Acid
Mo	Molybdenum
LoC	Lab-on-a-Chip
MY	Macrolex® Fluorescent Yellow 10GN
OPD	Optical Path Difference

Introduction and Research Aim

Our planet is facing significant changes due to warming^{1,2} and various anthropogenic disturbances³, such as pollution. These factors contribute to biodiversity loss⁴ and increased variability within ecosystems⁵⁻⁷. Given these challenges, it is crucial to understand how ecosystems react and respond, ideally by identifying generalizable principles that underpin the functioning of life and explicitly account for variability across scales. Metabolism⁸ serves as a suitable readout in this context, as it determines the demands organisms place on their environment while setting binding constraints on their energy allocation for survival, growth, and reproduction^{9,10}. In other words, metabolism sets the pace of life^{11,12}. Therefore, characterizing the metabolic rate of organisms under disturbances can be a universal and effect-based assessment of the impact of disturbances.

Many studies have explored global or regional disturbances and their impacts on species¹³, populations¹³, communities¹⁴ and ecosystems¹⁵, such as marine deoxygenation, acidification^{14,16} and warming^{13,15}. However, the detailed patterning of these dynamic changes at finer levels, such as chemical flows near or within biological structures in aquatic environments, remains technically limited, thereby constraining deeper studies on how disturbances influence individuals' bioprocesses such as metabolic activities. Understanding these individual bioprocesses in response to environmental changes is essential for more precisely elucidating how larger-scale environmental changes impact the metabolic health and overall resilience of marine ecosystems¹⁷. In **Paper I**, O₂-sensitive optode microparticles, along with an advanced microscope imaging system, were applied to develop a technique that can track spatiotemporal O₂ fluxes at microscales. This technique was then utilized by our collaborator to visualize O₂ transport near the surface of coral segments and found that cilia movements transport O₂ to optimize coral respiration.

Metabolism, as the "pacemaker" across all taxa, has been the key element in developing generalizable theories for entire ecosystems. Resulting metabolic theories, such as dynamic energy budget theory^{18,19}, temperature-size rule^{20,21} and scaling theory^{22,23}, adeptly link the performance of individual organisms to the ecology of populations, communities, and ecosystems by accounting for

variations in metabolic rates and biochemical pathways across different organisms and environmental conditions. Among these theories, metabolic scaling theory has emerged as one of the most significant and widely studied principles due to its simplicity and universality in entire ecosystems. Scaling theory incorporates a fundamental physical constraint of geometrical size/mass and statistically describes how organisms' metabolic rates R scale allometrically with their body geometrical size/mass M , following the relationship $R \propto M^b$. One widely used interspecific scaling exponent b value is $3/4$, some researchers also advocate for a value of $2/3$ ^{24,25}. The predictive scaling exponent helps predict how changes at the smaller and individual level will affect larger-scale ecological processes. Recent research has highlighted the importance of scaling theory as a tool for assessing and predicting the impacts of environmental changes and disturbances across different organizational levels, from single-cells to entire ecosystems²⁶.

Among ecosystems, the marine environment is particularly challenged by warming²⁷ and anthropogenic activities³. These large bodies of water are major sinks for atmospheric carbon dioxide (CO_2) and significant sources of oxygen (O_2), as phytoplankton perform half of the photosynthesis on Earth²⁸. Consequently, the marine 'biological carbon pump' plays a vital role in the net transfer of CO_2 from the atmosphere to the deep ocean and sediments²⁹. The efficiency of this biological pump is influenced by the metabolic prowess of phytoplankton and the performance of their community, which are governed by the physical and chemical conditions of the water bodies²⁹. The uptake and transfer of resources in marine ecosystems are thus directly connected to the metabolic abilities of individual phytoplankton cells. Therefore, characterizing the metabolic activity of phytoplankton is crucial for studying the effects of changes and disturbances in marine ecosystems. One of the objectives of this thesis was to quantify the metabolic rates in phytoplankton and examine how these rates change under different chemical conditions (**Paper III**). Diatoms were chosen as the phytoplankton model species because they often dominate phytoplankton communities and are very strong competitors among phytoplankton in marine ecosystems²⁹⁻³¹. Additionally, their unicellular nature satisfies the needs for single-cell levels studies in metabolic scaling theory (**Paper IV**).

However, traditional approaches that characterize organismal metabolic activity rely on bulk techniques, which tend to obscure differences among individual cells and provide only an integrated signal. While some single-cell characterizations of phytoplankton physiology exist, such as the cellular O_2 respiration measurement via O_2 -sensitive optical sensors^{32,33}, technical challenges in conducting high-throughput measurements and data processing remain significant. To achieve high-throughput, time-resolved analysis of metabolic rates of individual cells, this thesis developed novel glass microfluidic systems

that enable measurements of single-cell O₂ respiration rate via the combination of immobilized O₂-sensitive optodes^{34,35} and gastight chambers³⁶, i.e. closed glass microwells in **Paper II-IV**.

Alongside the optical measurement of cellular dry mass via quantitative phase imaging (QPI)³⁷, this allowed for a more accurate quantification of body mass compared to standard geometrical size measures, including area (**Paper II**), length, or volume. The combined analysis of cellular O₂ respiration and dry mass across three different phytoplankton species with varying dimensions (16 - 300 μm) was realized in **Paper IV**. This joint measurement was integrated into a scaling framework to gain insights into the linkage between single-cell variability, and inter-species levels of phytoplankton.

Beyond applications in ecosystem studies, scaling theory plays a crucial role in toxicological and pharmacological research, such as in the extrapolation of the human equivalent dose (HED) from smaller animal or tissue/organ models^{38,39}. **Paper II** aimed to apply cellular metabolism and geometrical size measurements on human hepatic cells. These joint single-cell measurements revealed size-related O₂ consumption kinetic parameters and cells' ability to adapt to local O₂ availability via changing respiration rates. This is crucial for understanding tissue function and has applications in developing therapeutic strategies.

Precisely controlling chemical dynamics in microenvironments that affect metabolism and other biological processes was also a key objective of this thesis. Manipulating chemical environments and mapping them near organisms is essential for studying environment-organism interactions in phytoplankton. In **Paper III**, an array of optode-decorated glass microwells was combined with a movable channel plate⁴⁰. This allowed for the horizontal "slipping" motion of the channel over microwells, the coordinated loading of single-cells, their exposure to chemicals and measurements of their O₂ respiration. This device, SlipO₂Chip, was used to measure the dose-dependent change of phytoplankton respiration rate under different levels of the bacterial quorum signal molecule 2-Heptyl-4-Quinolone (HHQ)⁴¹.

Overall, the development of these microfluidic approaches enables precise measurement of O₂ at microscales, including the visualization of spatiotemporal O₂ dynamics at the microscale and the characterization of intracellular O₂ metabolism under chemical changes.

The scope of the thesis is summarized in the following points:

- I. To develop and demonstrate chemical sensing particle image velocimetry (sensPIV), a method to simultaneously measure O₂ distributions and flow fields via optode microparticles (**Paper I**).
- II. To develop microfluidic devices for measuring cellular O₂ respiration rates in individual and multiple mammalian cells (**Paper II**) as well as single phytoplankton cells (**Paper III and IV**).
- III. To study the size-related variability in O₂ consumption kinetics of single and O₂ availability-limited adaptively changing respiration rates (**Paper II**).
- IV. To perform single-cell O₂ respiration measurements in phytoplankton cells before and after chemical exposures by developing SlipO₂Chip device (**Paper III**).
- V. To combine cellular O₂ respiration measurements with dry mass measurements in three model phytoplankton species of varying cell sizes and integrate the data into scaling theory (**Paper IV**).

Summaries of the aforementioned papers are provided in Chapter 5.

Chapter 1: Microscale O₂ Fluxes and Cellular O₂ Metabolic: Insights into Bioprocesses

O₂ fluxes in microenvironments

O₂ is a key environmental factor influencing numerous biological processes. At the cellular level, O₂ is essential for aerobic respiration, a process in which cells convert glucose into adenosine triphosphate (ATP), the primary energy currency. This process, known as the electron transport chain (ETC), occurs in the mitochondria and is highly efficient in energy production⁴². Adequate O₂ levels enable cells to maintain metabolic functions, grow, and proliferate, while low O₂ levels force cells to switch to anaerobic metabolism, leading to less efficient energy production and lactate accumulation⁴³.

In aquatic systems, small organisms such as bacteria, algae, and corals exhibit various responses to O₂ availability which are dynamically changing with water flow, affecting both their metabolic processes and interactions within communities. One widely studied case is marine hypoxia, defined as dissolved O₂ at a concentration of less than 2.8 mg O₂/L⁴⁴, which has been increasing due to warming-induced O₂ solubility decrease⁴⁵ and anthropogenic eutrophication like agriculture, sewage, and fossil fuel combustion⁴⁶. Studies show that hypoxia triggers diatoms' lipid utilization, modifies metabolic pathways, and activates stress resistance mechanisms to adapt to low O₂ conditions⁴⁷ as well as directly inhibits diatom growth^{47,48}. Diatoms serve as important primary producers²⁹ and changing O₂ availability has thus the potential to significantly impact global carbon^{29,49} and silica⁵⁰ cycles within marine ecosystems. Additionally, dissolved O₂ levels have been considered among the main drivers causing shifts in bacterial community interactions and functions⁵¹.

Global and regional changes such as hypoxia caused by seasonal temperature fluctuations or nutrient cycles, have been extensively documented through in situ sampling/monitoring^{52,53} or remote sensing^{54,55}. However, investigating microscale O₂ fluxes, such as advective and diffusive O₂ fluxes near or within coral, algae, and even bacteria, is often limited by technical constraints. Movable optical fibers have been used to probe the spatiotemporal distribution of O₂ in hepatic engineered tissues⁵⁶ and hydrogel-encapsulated algal⁵⁷. But the resolution of this method is restricted by the size of the optical fiber and that

of mechanical stages, making it unsuitable for measuring very small organisms at a realistic throughput. In **Paper I**, sensPIV was developed to address these limitations. Based on the principle of particle image velocimetry (PIV), a method used to visualize fluid flow via particles⁵⁸, sensPIV combines O₂-sensitive optode micro-particles and a rapid imaging microscope to simultaneously track O₂ concentrations and flow fields in microscale environments, such as cilia facilitated O₂ transport above the surface of corals⁵⁹.

SensPIV is non-invasive and utilizes microscope imaging, making it also suitable for integration with microfluidic devices. Therefore, beyond marine biology, sensPIV has significant potential in biomedical research, particularly in the development and use of in vitro microfluidic models (organ-on-a-chip⁶⁰), which are increasingly important in this field. O₂ flux is a critical factor in these organ/tissue/cell cluster models, as O₂ delivery and availability influence cellular metabolic states and the functioning of tissues and organs. Insufficient O₂ supply at the tissue or cellular level can activate hypoxia-inducible factor-1, allowing cells to avoid ATP depletion, senescence^{61,62} and cell death⁶³. Conversely, hyperoxia can lead to decreased ATP levels, senescence, and cell death without hypoxia-inducible factor-1 activation, mediated by mitochondrial-derived reactive oxygen species (ROS)⁶³. By applying sensPIV in such in vitro models, researchers could thus monitor and regulate O₂ levels in tissues and organs more precisely. This knowledge could help address questions such as how O₂ transport in tissues affects wound healing and cancer progression, given that hypoxic conditions can promote tumor growth and resistance to therapy⁶⁴, or to help understand the pathophysiology of the intestine models, where hypoxic environments are critical for nutrient absorption, intestinal barrier function, and innate and adaptive immune responses in the mucosal cells of the intestine⁶⁵.

O₂ metabolism in toxicological studies

O₂ production and consumption are also fundamental indicators of metabolic activity, reflecting an organism's energy expenditure on physiological processes such as growth, reproduction, and survival⁸. Conversely, photosynthetic organisms, such as algae, produce O₂ as a by-product of photosynthesis, which is equally crucial for their metabolism. Therefore, the rate of O₂ consumption and production can be directly correlated with the overall metabolic rate of a cell or organism. Studies have shown that O₂ uptake and production provides a quantifiable measure of the energy expended and produced during metabolic activities^{66,67}.

O₂ as an effect-based marker of chemical effects

Toxic substances can disrupt normal cellular metabolism, leading to adverse effects on cell function and viability. Mitochondria are crucial for many metabolic processes, such as energy production, regulation of apoptosis, synthesis of macromolecules, and generation of intracellular messengers such as Ca²⁺ and ROS⁶⁸. Therefore, many processes in mitochondria can be disrupted and this makes mitochondria a frequent target of chemical toxicity⁶⁸. One of the main mechanisms⁶⁹ causing mitochondrial dysfunction, is the inhibition of ETC which causes reduced O₂ consumption by chemicals like strobilurin herbicides⁷⁰. Another mechanism is the uncoupling of oxidative phosphorylation in which the proton gradient across the mitochondrial membrane is disrupted. An exemplary chemical compound causing such disruption is the herbicide bromoxynil⁷¹. Mitochondrial dysfunction results in reduced O₂ consumption and ATP synthesis leading to cellular energy deficits. Given the central role of O₂ metabolism in cellular health, O₂ consumption rates (OCR) can serve as a real-time, effect-based markers for assessing mitochondrial toxicity. Decreased O₂ consumption rates might signal impaired mitochondrial respiration, while increased rates could reflect a compensatory response to maintain ATP levels despite mitochondrial damage. Researchers have used OCR to assess mitochondrial metabolism and toxicity of chemicals in a wide range of organisms and cells: zebrafish embryos⁷², *Caenorhabditis elegans*⁷³, liver cells^{68,74,75} and cardiomyocytes⁷⁶. These studies have helped uncover toxicological mode of actions and aided in the formulation of effective mitigation strategies.

In addition to well-known anthropogenic chemicals like herbicides, the toxicity of natural metabolites also requires attention. For instance, secondary metabolites^{77,78} are organic compounds that are not directly involved in the normal growth, development, or reproduction of organisms. Instead, they often play crucial roles in defense mechanisms, competition, and signaling within ecosystems. One such secondary metabolite is HHQ, a quorum sensing (QS) molecule secreted by bacteria and can be commonly found in water systems and soil⁷⁹. HHQ is used to coordinate behavior based on population density⁸⁰. Beyond its impacts within bacterial communities, research has shown that HHQ can reduce photosynthesis and mitochondrial respiration in diatoms, thereby suppressing their growth at nanomolar concentrations⁷⁹. This suggests that the bacterial QS molecule HHQ can affect diatom physiology and such bacteria-diatom interactions could have outsized impacts on diatom blooms^{81,82}. Experimentally verifying the toxicity of HHQ on diatom respiration is thus crucial for understanding its potential environmental impact. Measuring OCR of unicellular diatoms can reveal cellular heterogeneity within populations, enhancing our understanding of classic dose-response

models with quantitative assessment of cell-to-cell heterogeneity. Thus, in **Paper II and III**, a micro-respiration chamber device was developed, consisting of gas-tight microwells and immobilized O₂-sensitive optode layers. This device enabled OCR measurement at the single-cell level. In **Paper III** the dose-response effect of HHQ on diatom respiration was established.

Notably, some chemicals also impair other cellular functions through mechanisms including increasing the production of ROS, leading to oxidative stress and DNA damage⁸³. While O₂ metabolism is a sensitive marker capable of detecting subtle changes in cellular function that may precede more overt signs of toxicity, this sensitivity allows for the identification of early-stage toxic effects and the potential implementation of interventions before significant damage occurs. To comprehensively study the toxic effects of toxicants and understand their long-term impacts, it is essential to complement O₂ metabolism measurements with other methods, such as genomic and proteomic analyses⁸⁴, cell viability⁸⁵ and apoptosis assays⁸⁶.

Application in metabolic scaling theory study

Metabolism, often considered the "pacemaker" across all taxa¹², plays a crucial role in the development of generalizable theories for entire ecosystems. Despite the vast range of organism sizes, spanning over 10²¹ orders of magnitude, metabolic scaling theory - a classical scaling theory - asserts that metabolic rates scale to a certain power of an organism's mass²². This relationship is expressed through the basal metabolic rate, which can be calculated using a power function: $R = aM^b$, where R is the metabolic rate, a is a constant that varies depending on the type of organism and environmental conditions, M is the body size, and b is a scaling exponent which is often close to 3/4 for many organisms²⁴.

The scaling theory unifies population, community, and ecosystem approaches by focusing on the ecophysiology of individual organisms⁸⁷. In this context, metabolism plays a fundamental role as the unifying concept these different organizational levels. Metabolic scaling theory provides insights into the relationship between organismal traits and ecological processes, helping us understand how changes in climate and environment might impact biodiversity and ecosystem function. Additionally, it offers a framework for examining energy distribution and resource use across different ecological scales, from individual organisms to entire ecosystems^{26,88}. For example, a straightforward linear relationship between the residence time of carbon molecules and the ratio of whole-ecosystem biomass can describe primary productivity⁸⁹. Furthermore, the scaling pattern is also crucial for toxicologists to extrapolate a HED from doses given to smaller model animals³⁸.

While many scaling theory studies generally holds an interspecific $b = 3/4$ across different species, this value has been debated with some research advocating for $2/3$ ^{23,25,90}. Moreover, it has been proposed that intraspecific scaling deviates from the "3/4 rule," emphasizing the differences between these two levels of scaling²⁵. Despite this, our comprehension of metabolic scaling within individual microorganisms and its relationship to population-level scaling is also limited⁹¹. A study⁹² in phytoplankton single-cells, the scaling exponents for carbon and nitrogen uptake rates relative to cell volumes were approximately 0.69 and 0.59, respectively. These values are lower than the traditional interspecific scaling exponent of $3/4$, commonly used in animal studies. This deviation might be attributed to several factors unique to microorganisms, such as their high surface-area-to-volume ratios, which influence nutrient uptake and metabolic rates. In **Paper II**, the developed micro-respiration chamber device was used to measure intracellular O_2 respiration and cell area of single human hepatic cells, focusing on the geometrical size-related and source-limitation-adapted O_2 respiration kinetics. Then in **Paper IV**, the inter- and intraspecific metabolic scaling of three unicellular diatom species was investigated by jointly measuring cellular O_2 respiration and cell dry mass.

Chapter 2: O₂ Measurement at the Microscale

In Chapter 1, the importance of measuring O₂ fluxes in the microenvironment and cellular O₂ metabolism is discussed. This chapter provides detailed methodologies for O₂ measurement at microscales.

Microfluidics: an overview

The precise manipulation and measurement of chemicals at microscales has been realized by microfluidics, a technology that enables the exact control of small amounts of fluids (10^{-9} to 10^{-18} L) via microscale structures such as channels and droplets⁹³. By leveraging the unique physical properties of fluids at the microscale, microfluidics allows for controlled experiments that are significantly more efficient than their macroscale counterparts, offering advantages in terms of reagent use, speed, and resolution.

A typical microfluidic setup includes complex networks of valves, channels, and chambers featured into substrates, designed for liquid operations such as mixing, separation, and detection. The precision and efficiency of microfluidics have revolutionized the study of biological processes by enabling the manipulation and measurement of chemical levels within tiny volumes, providing unparalleled control over the microenvironment.

Microfluidics effectively "downscales" studies in various fields such as biology, pharmacy, and materials science, allowing researchers to conduct experiments at the microscale with significant advantages over traditional bulk methods. For example, microfluidics has been used to cultivate cells⁹⁴, encapsulate and deliver drugs in a targeted fashion⁹⁵, diagnose diseases⁹⁶, and prepare nanoparticles⁹⁷.

In this thesis, microfluidics was utilized to provide well-controlled chemical conditions, manipulate single-cells, and characterize cellular O₂ metabolism in highly controlled settings. Key elements relevant to the thesis work include the immobilization of cells, the use of microwells and channels to maintain and perturb these cells, and the imaging systems required to visualize these processes. Various materials and fabrication techniques are employed to meet

specific experimental requirements, emphasizing the balance between feasibility, biocompatibility, and cost-effectiveness. These aspects will be introduced in the following sections.

Materials and fabrications of microfluidic devices

Microfluidic devices leverage a variety of materials, including silicone-based polymers, glass, and various plastics, to form intricate microscale channels and chambers. These materials are chosen for their compatibility with a wide range of chemical and biological substances. Fabrication techniques range from the simplicity and cost-effectiveness of photolithography⁹⁸ and soft lithography⁹⁹, particularly favored for device fabrication via polydimethylsiloxane (PDMS), glass and silicon etching¹⁰⁰. More complex methods like 3D printing for plastics such as inkjet and 2-photon printing^{101,102}, facilitate rapid prototyping and scalable production¹⁰³.

The selection of material and fabrication method is critical, requiring a balance of feasibility, biocompatibility, and integration with other measurement technologies. The following sections detail the materials used and the corresponding fabrication techniques employed in this thesis, illustrating how these choices enable the creation of sophisticated microfluidic systems tailored to various experimental requirements.

PDMS

PDMS is a silicone-based polymer widely used in microfluidic device fabrication for its excellent optical clarity and gas permeability, which are essential for biological applications¹⁰⁴. To construct PDMS microfluidics devices¹⁰⁵, a solution consisting of a silicone elastomer base and a cross-linking agent (usually a curing agent) was mixed together. The mixture was then poured over a master mold and cured by heating, typically at 60-80°C for several hours. This curing process facilitated a hydrosilylation reaction, where the vinyl groups on the silicone elastomer base reacted with the hydride groups on the curing agent, forming an elastomeric replica of the mold. The resulting PDMS replica can be permanently bonded to glass surfaces by treating both the PDMS and glass with O₂ plasma, which activated the surface by creating silanol groups. When pressure was applied, these silanol groups form covalent Si-O-Si bonds, creating a strong, permanent seal (Figure 1).

Master molds used in the thesis were created using photolithographic techniques (Figure 1), where a photoresist (SU-8)-coated silicon wafer was selectively exposed to UV light through a patterned photo mask - designed using AutoCAD and printed commercially. After UV exposure, the unexposed SU-

8 was developed in an organic solvent that removes the unexposed photoresist, leaving a relief structure that forms the microfluidic channels.

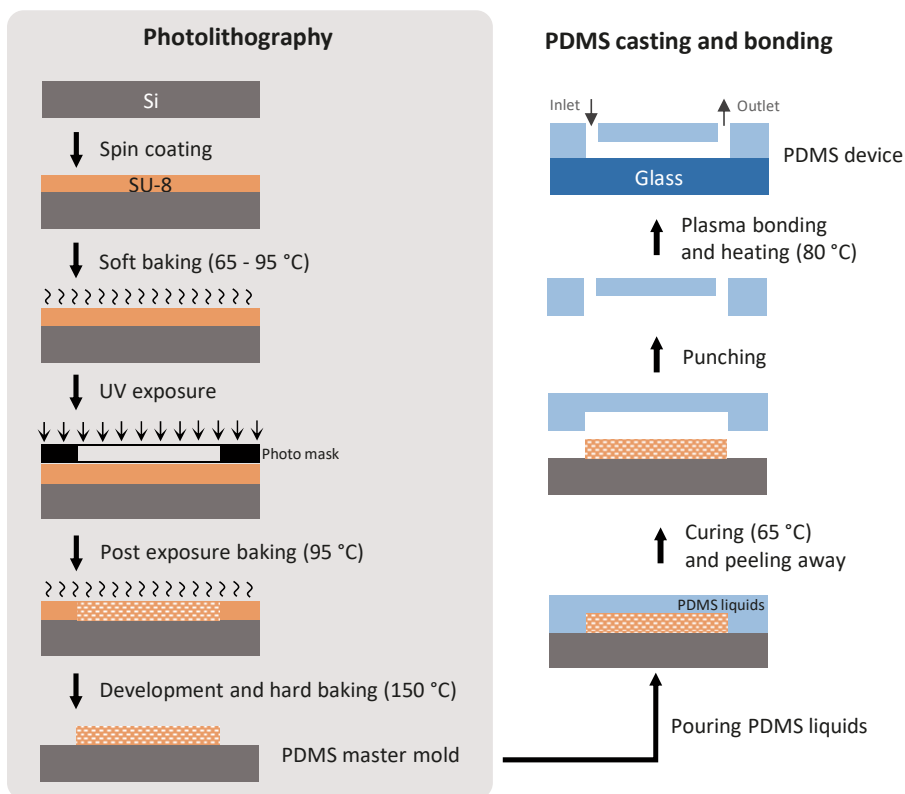


Figure 1 Schematics of PDMS microfluidic device fabrication. A PDMS master mold featuring microstructures is first fabricated using a silica wafer and photoresist SU-8, following photolithography steps. Then PDMS mixture liquids was poured onto the master mold. After curing, PDMS solidified and can be peeled away from the mold. The PDMS piece was then cut, and holes were punched for inlets and outlets. Following O_2 plasma treatment, the PDMS piece was bonded onto a glass surface, forming the PDMS microfluidic device with the desired microstructures.

Paper I presents a PDMS microfluidic system (Figure 2) involving a main fluidic channel flanked by two gas channels, where nitrogen gas (N_2) and compressed air (CA) were introduced respectively create controlled O_2 gradients and a laminar flow in the mid-channel. This setup enabled the testing of Pt(II) meso-Tetra(pentafluorophenyl)porphine (PtTFPP) microparticles in tracking and quantifying well controlled spatiotemporal O_2 dynamics, demonstrating the effectiveness of the sensPIV system for more complex measurements.

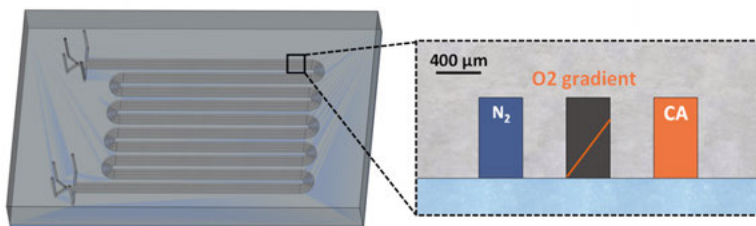


Figure 2 Solid view of the three-channel PDMS device used in **Paper I**, and the channel cross-section. The two side channels were introduced with N_2 and CA gases respectively. A linear O_2 gradient was generated in the central channel due to the gas permeability of PDMS, allowing for the testing of sensPIV performance in measuring well-controlled chemical fluxes.

Glass

Glass is an excellent material for microfluidic devices due to its gas-impermeability, chemical inertness, and superior optical properties¹⁰⁶, making it ideal for precise measurements of cellular O_2 dynamics and exposure to toxicants. In our work, we utilized two glass etching techniques to fabricate microfluidic devices, each chosen based on the desired resolution and application:

(1) Dry etching

Dry etching involves creating recessed microstructures in glass using a reactive ion etching (RIE) machine that employs ionized gases like SF_6 to selectively remove material from the glass surface^{100,107}. The process began by sputtering an aluminium (Al) layer onto the glass, followed by applying a photoresist layer through standard photolithography techniques. The Al layer was then etched using an inductively coupled plasma-reactive ion etching (ICP-RIE) machine with Cl_2 and BCl_3 gases. In the final RIE etching step, glass is selectively etched under the protection of the Al mask. This protocol (Figure 3A) achieved high-resolution microstructures down to $0.1 \mu m$ and resulted in a maximal etching depth of approximately $55 \mu m$, with a depth-proportional etched arithmetic average roughness (Ra), defined as the absolute average relative to the base length, of about 2200 nm at $55 \mu m$ depth. Although being time-intensive and expensive, the precision and anisotropy of dry etching make it widely used for creating fine features (Figure 4A). In **Papers II – IV**, microwells diameter (\emptyset) ranging from $50 \mu m$ to $200 \mu m$ were etched for the immobilization of single-cells of difference sizes.

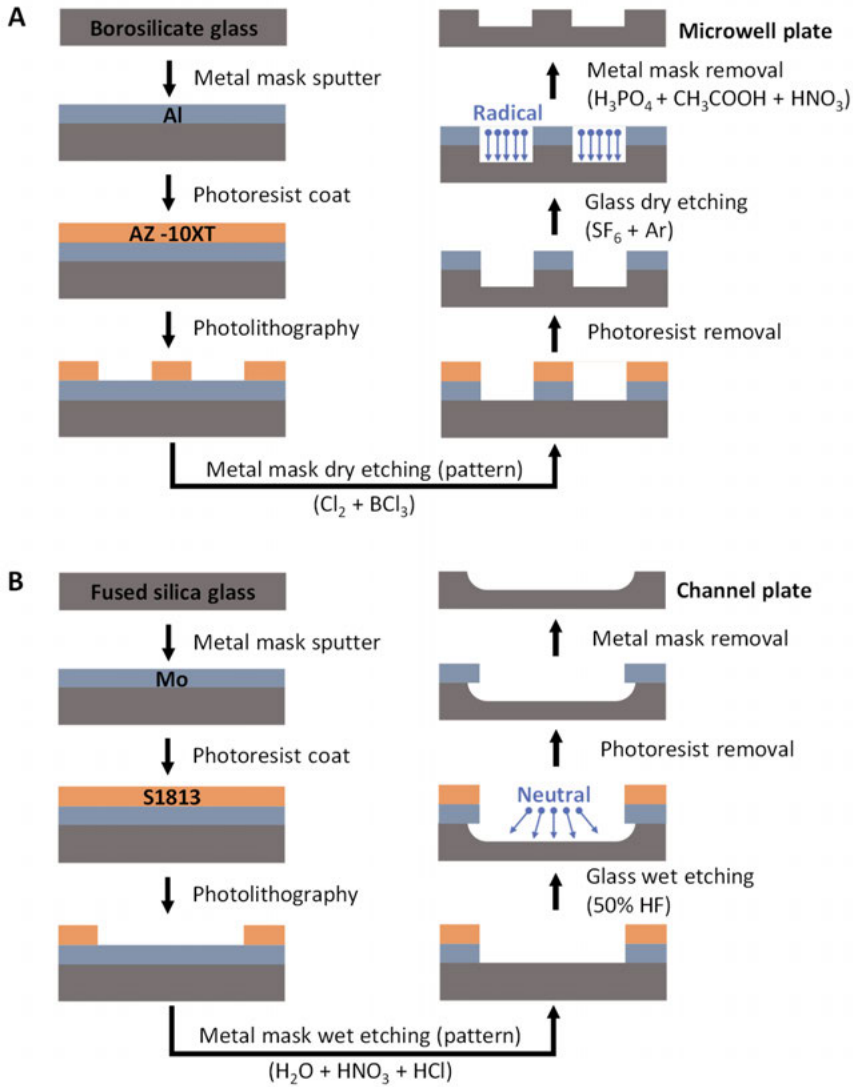


Figure 3. Schematics of dry etching and wet etching of glass. **(A)** Deep reactive ion etching (DRIE) of borosilicate glass was carried out using SF₆ and SF₆/Ar plasma. Sputtered Al on the glass structure using patterned AZ-10XT photoresist mask was used as a hard-mask for plasma etching. **(B)** The wet etching of fused silica glass was carried out using 50% HF acid. Sputtered Mo on the glass structure using patterned S1813 photoresist mask was used as a hard-mask for the wet etching.

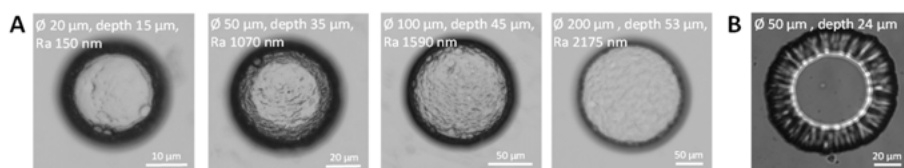


Figure 4 Comparison of dry etched and wet etched glass patterns, in the example of microwell structure. **(A)** Dry etched microwells with diameters from 20 μm to 200 μm and varied depth from 15 μm to 53 μm . The etched surface roughness increases with depth. Microwell walls are vertically straight. **(B)** A wet etched microwell with a diameter of 24 μm and a depth of 24 μm . The microwell bottom is smooth and the microwell opening is widened due to the isotropic nature of wet etching.

(2) Wet etching

Wet etching (Figure 3B) utilizes liquid chemicals like hydrofluoric acid (HF) to chemically etch the glass surface^{108,109}. Due to the amorphous nature of glass, this process is isotropic, etching uniformly in all directions (Figure 4B). It requires a metal mask for patterning, typically molybdenum (Mo), which was sputtered onto the glass. A photoresist layer is then added for generating the Mo mask through the Mo patterning step. Then the glass wafer with the Mo mask was immersed in HF for the glass wet etching. Wet etching is faster than dry etching and generate smoother etching surface but does not achieve resolutions finer than 1 μm . It is best suited for constructing larger channel structures, from millimeters to centimeters, as utilized in the channel fabrication in **Paper III**, which don't require vertical walls and precise shapes.

Lab-on-a-Chip: integration of microfluidics with O₂ measurements

Expanding on the foundational technology of microfluidics, the concept of Lab-on-a-Chip (LoC)¹¹⁰ integrates multiple laboratory functions into a single microfluidic chip. Essentially, LoC systems are miniaturized versions of traditional laboratory setups, designed to perform complex assays within a compact, automated platform. They incorporate various stages of a complete laboratory procedure, including sampling, sample pretreatment, chemical reactions, product separation, isolation, detection, and data analysis. To achieve this, LoC devices utilize miniaturized components such as filters, pumps, valves, actuators, heaters, motors, and integrated detection systems like optical and electric sensors, and additional analytical techniques such as capillary electrophoresis, chromatography, and mass spectrometry, significantly enhancing their utility. These integrations allow for efficient, high-throughput analysis, making LoC systems a powerful tool in scientific research and diagnostics^{111,112}.

In this thesis, a significant innovation is the integration of O₂-sensitive optical sensors and a microscope imaging system in LoC systems for the purpose of measuring O₂ dynamics at microscale.

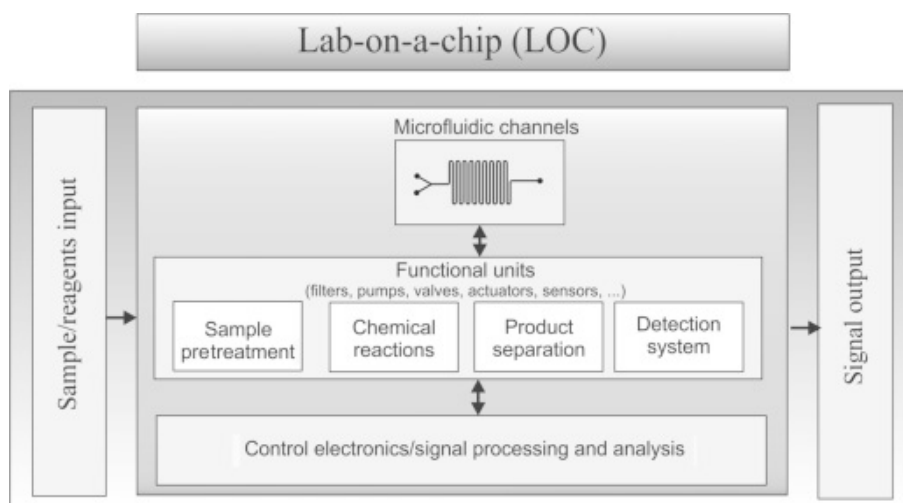


Figure 5. Components of Lab-on-a-Chip. Copyright © 2019 Elsevier. Reprinted with permission from reference 111.

O₂-sensitive optode sensors

O₂ measurement in LoC systems can be accomplished through various methods, including electrochemical and optical sensors¹¹³. Electrochemical sensors, such as Clark-type electrodes, are widely used in LoC applications, such as O₂ sensing in cell cultures¹¹⁴ due to their sensitivity and fast response capabilities. However, they often require calibration and can consume O₂ during measurement, potentially affecting the microenvironment¹¹⁵. Optical sensors, or optodes, offer a non-invasive alternative, utilizing the principles of luminescence quenching to detect changes in O₂ levels^{116,117}. Unlike electrochemical sensors, optodes do not consume O₂ and provide the added benefit of spatial resolution of O₂ measurement by applying different optodes types such as immobilized planar and moveable micro/nano-particle³⁴. Optodes are particularly valued for their ability to integrate with imaging systems, enabling real-time, high-resolution monitoring of O₂ dynamics across various experimental conditions and scales, from plant roots¹¹⁸ to single-cells (**Paper II - IV**). This adaptability makes them highly suitable for complex biological assays where understanding O₂ dynamics is critical.

(1) Composition, measurement and applications

The O₂-sensitive optodes used in this thesis consist of a luminescent dye, PtT-FPP, whose optical properties are reversibly influenced by the presence of

molecular O₂, and an O₂-insensitive reference dye, Macrolex® fluorescent yellow 10GN (MY). When exposed to light of a specific wavelength (365 nm), the PtTFPP dye absorbs photons and becomes excited. In the absence of O₂, the indicator dye returns to its ground state by emitting a photon, resulting in luminescence (red light 650 nm). However, in the presence of O₂, the excited dye molecules transfer energy to O₂ molecules, quenching the luminescence in a process that can be quantitatively measured¹¹⁹.

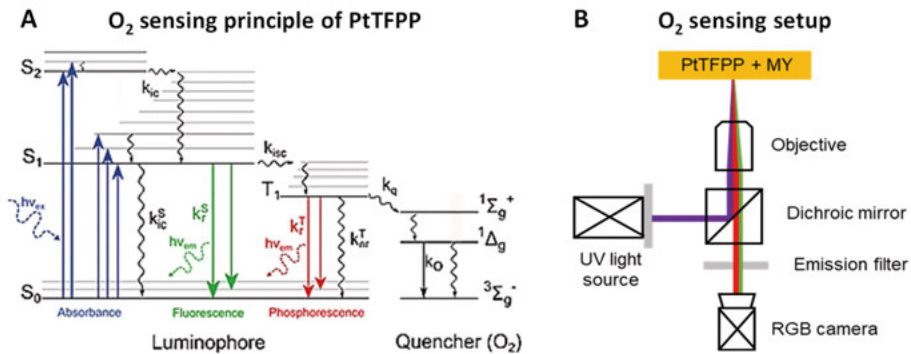


Figure 6 Working principle and imaging system of O₂-sensitive optodes. **(A)** Perrin-Jablonski diagram describing the working principle of O₂ optodes based on the luminescence quenching by O₂. Copyright © 2012 Michela Quaranta et al. Reprinted with permission from reference 35. When optodes are exposed to UV light, the luminescent molecule absorbs photons and become excited from its ground state (S₀) to a higher electronic state (S₁ or S₂). From this excited state, two major de-excitation processes are possible: fluorescence emission and phosphorescence emission. Both emissions lead to light emitted at a longer wavelength compared to the absorbed light (= Stokes' shift). In the presence of molecular O₂, the photoluminescence of such molecules is quenched through the molecular interaction between the quencher (= O₂) and the luminophore. This process is diffusion limited. The whole reaction occurs in about 10⁻¹² s. **(B)** Experimental imaging setup used in experiments to perform ratiometric O₂ measurements. UV light is provided via a SpectraX tunable light source. The O₂ sensor consisting of the optode material PtTFPP and indicator dye MY is excited by UV light and its luminescence emission redirected by the dichromatic mirror. Images are acquired by an RGB camera mounted and automatically triggered by an automated epifluorescence microscopy platform. The RGB image is subsequently split up into its individual red and green signals to perform ratiometric imaging.

This relationship between O₂ concentration and red emission intensity is described by the Stern-Volmer equation (Equation 1)³⁵. Herein, I_{red} is the luminescence intensities of red emissions in the presence of O₂, being a function of O₂ concentration [O₂] (% air saturation); $(I_{red})_{0\% \text{ air saturation}}$ denotes the red luminescence intensities in the absence of O₂; k_{SV} represents the Stern-Volmer constant.

$$\frac{(I_{red})_{0\% \text{ air saturation}}}{I_{red}} = 1 + k_{SV} [O_2] \quad \text{Equation 1}$$

Under the same UV excitation light, the MY dye emits green fluorescence and is O₂-insensitive (~512 nm)¹²⁰. By performing a ratiometric measurement of the red/green intensity of the optodes and reference dye, the O₂ concentration can be related to the intensity ratio. This method compensates for uneven illumination as well as the positional heterogeneity of the optode amounts, as the emission light intensity depends on both O₂ concentration and optode density. And the Stern-Volmer equation is adapted into Equation 2, where $(\frac{I_{red}}{I_{green}})_{0\% \text{ air saturation}}$ and $\frac{I_{red}}{I_{green}}$ signify the ratio of luminescence intensities between the red and green channels in the absence and in the presence of O₂, respectively.

$$\frac{(\frac{I_{red}}{I_{green}})_{0\% \text{ air saturation}}}{\frac{I_{red}}{I_{green}}} = 1 + k_{SV} [O_2] \quad \text{Equation 2}$$

To immobilize or encapsulate PtTFPP and MY dyes, biocompatible and O₂-diffusible polystyrene is used as a matrix to prepare different types of optodes like micro/nano-particles and planar sensors¹²¹ (Figure 7). For micro/nano-particles preparation, aqueous surfactant solution and vigorous stirring steps are additionally required¹²². These particles are ideal for *in situ* measurements in tight spaces and complex matrices, such as rough coral surfaces and within cellular clusters or tissue^{123–126}, where traditional sensing methods may be invasive or disruptive. The micro-particle optodes used in **Paper I** were provided by Koren Lab at Aarhus University.

To prepare planar optodes, the same mixture solution is used, with silicone rubber added to improve adhesion¹²⁷. The mixture is homogeneously spread onto support surfaces and dries out becoming planar optodes in LoC devices, such as near cell clusters to measure O₂ gradients¹²⁸, or at the bottoms of encapsulated microwells for cellular O₂ consumption measurement (**Paper II – IV**). Additionally, planar sensors enable 2D imaging of O₂ distributions, providing insights into O₂ heterogeneity within complex biological samples, such as the sediment-water interface^{129–131}, plant tissues¹³², corals¹³³ or cell cultures¹²⁸.

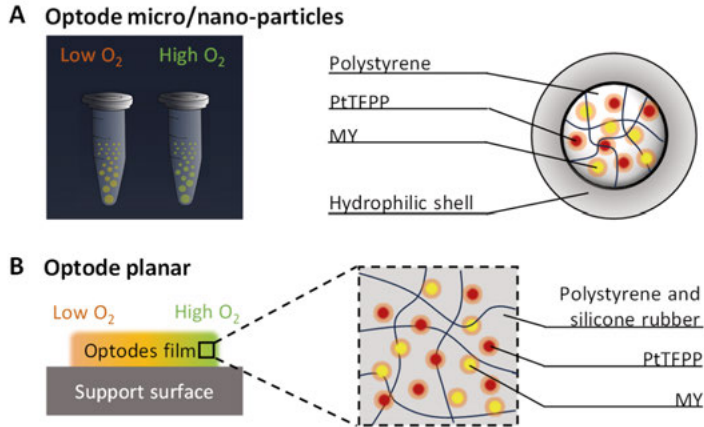


Figure 7 Two types of O_2 -sensing optodes used in Lab-on-a-Chip systems: micro-particle and planar optodes. Both optodes are typically composed of an O_2 -sensitive luminescent dye, PtTFPP, and a reference dye MY, encapsulated within a polystyrene matrix. **(A)** Micro/nano-particle optodes. **(B)** Planar optodes decorated on a support surface.

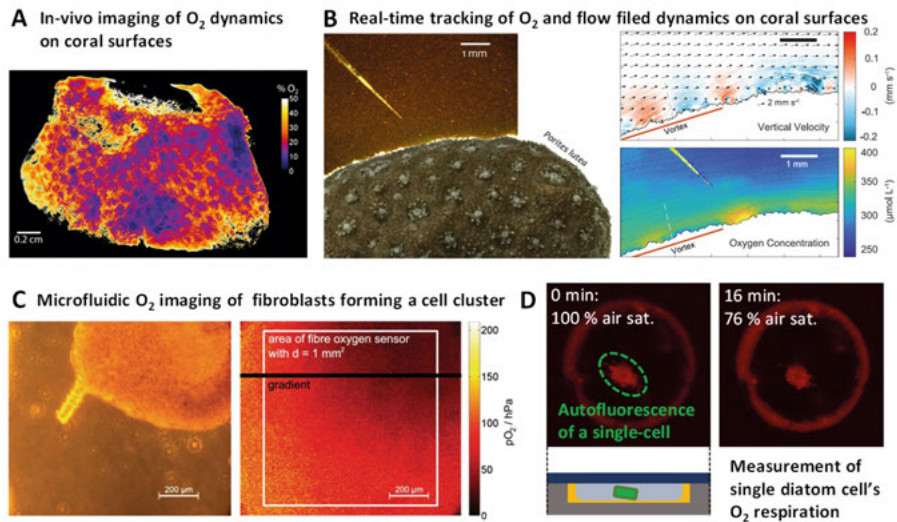


Figure 8 Example applications of O_2 -sensitive micro/nano-particle and planar optodes. **(A)** In-vivo imaging of O_2 distribution on the surface of a coral fragment spray-painted with optode nanoparticles. Copyright © 2016 Elsevier B.V.. Reprinted with permission from reference 134. **(B)** Real-time characterization of the spatial-temporal dynamics of O_2 and flow fields near coral surfaces via optode microparticles (**Paper I**). **(C)** Microfluidic O_2 imaging using integrated optical sensor layers and a color camera. Copyright © 2013 The Royal Society of Chemistry. Reprinted with permission from reference 128. **(D)** Measurement of single-cell O_2 respiration with immobilized planar optodes in gas-tight chambers (**Paper II and III**).

The design and choice between particle and planar optodes depend on the specific applications, such as the need for spatial resolution, sensor invasiveness, and the environment being studied (Figure 8).

(2) Readout and data processing

The O₂ sensing setup in Figure 6B enables the quantification of local O₂ concentrations using an RGB camera. This is achieved through the analysis of O₂-sensitive red and reference green light emissions, allowing accurate determination of O₂ levels based on the ratiometric measurement adapted Stern-Volmer relationship (Figure 9).

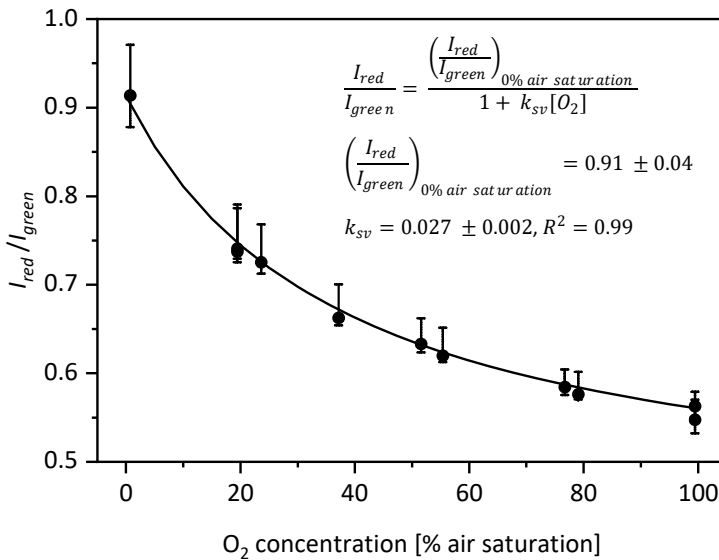


Figure 9. The O₂ dependent luminescence quenching of a typical optodes, PtTFPP, calibrated in the ratiometric manner. The kinetics of collisional quenching of optodes luminescence by O₂ is well described by the Stern–Volmer equation. This diagram displays an optodes calibration example describing the reduction in luminescence in response to O₂ presence, where k_{SV} and the ratio I_{red}/I_{green} at 0% air saturation adjust based on various parameters like UV light power, exposure duration, and optode density.

The thesis demonstrates the application of PtTFPP micro-particle optodes for simultaneous measurements of fluid dynamics and chemical exchange processes (**Paper I**) and the use of optode coated microwells for measuring single-cell O₂ consumption (**Papers II and III**).

In **Paper I**, sensPIV particles were individually segmented and tracked using the TrackMate (version 4.0.0) plugin in ImageJ (version 1.8.0), enabling dynamic monitoring of spatial and temporal O_2 fluctuations. In **Papers II** and **III**, RGB image stacks were analysed to measure intensity ratios between the red and green channels, from which local O_2 concentrations were calculated. This image processing was done using Fiji Image Processing (version 2.0)¹³⁵ and Matlab (version 2020b, Mathworks).

Quantitative Phase Imaging (QPI)

QPI¹³⁶ is a label-free imaging method that can be used to calculate a living cells' dry-mass by measuring refractive index changes¹³⁷. As light passes through a transparent object, different parts of the specimen, with different thickness and distinct refractive indices, generate slight changes in the phase of the propagating light wave. These slight phase changes enable to calculate the object's optical volume and thus dry mass with a density. Experimentally, this requires taking two images, one consisting of a cell-free area ('reference') and another that contains the cells of interest. The combination of both images enables computing the cell-derived phase shifts, the measurement of the optical volume of cells which together provide information about cellular dry-mass.

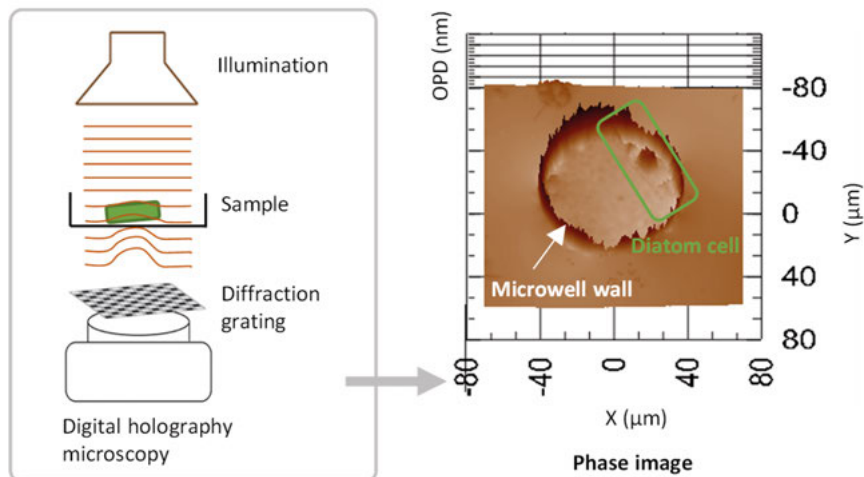


Figure 10. Quantitative phase imaging (QPI): dry mass measurement of a single-cell isolated in a microwell with digital holography microscopy. Figure is adapted from reference 138. To measure the optical wavefront of light diffracted by the sample, an interference pattern is recorded using reference light with a known wavefront. This phase information is then converted into a fringe pattern, forming a hologram. Computational field retrieval algorithms extract both the amplitude and phase of the measured light from the hologram. For a single diatom cell isolated in a glass microwell, the retrieved field information creates a phase-delay map, which is caused by the refractive index difference between the cell and its surrounding medium.

The calculation of cell dry mass is described by Equation 3 below. In this equation, x and y are the two-dimensional coordinates of the imaging field. The term $\Delta\phi(x, y)$ denotes the phase shift at each point (x, y) in the cell. λ stands for the wavelength of the light used, and the factor 2π converts the phase shift, measured in radians, into optical path difference (OPD), with OPD defined as $\frac{\lambda}{2\pi} \Delta\phi$, expressed in units of length. α is a proportionality constant that relates the refractive index increment to the mass density of the cell, typically $\alpha = 0.185$ mL/g for many biological cells¹³⁹. This equation integrates the phase shifts across the cell area to determine the total dry mass.

$$M = \frac{\lambda}{2\pi \cdot \alpha} \iint \Delta\phi(x, y) dx dy \quad \text{Equation 3}$$

The superior optical properties of the glass material used in the micro-respiration chamber device constructed for measurements in **Paper II** also allow for joint measurement of cellular O₂ respiration and dry mass on the same cells, as demonstrated in **Paper IV**. These combined measurements were carried out on three unicellular diatom species ranging from 16 to 300 μm . The primary data obtained has been used to fit into the classic scaling theory.

Verification

Verification is a crucial aspect of developing and implementing microfluidics and LoC technologies. Ensuring the accuracy and reliability of these devices is essential, as they often serve complex biomedical and environmental monitoring purposes. Rigorous verification processes not only confirm the functionality and performance specifications but also enhance the credibility of the technologies for academic, clinical, and industrial applications. This involves systematically comparing experimental data with theoretical models to bridge the gap between design and practical utility.

In **paper I**, the accuracy of observed O₂ transport in a PDMS device was verified using a combination of numerical modeling and experiments. Multiphysics COMSOL, a finite element software suite, was employed to simulate real-world designs, devices, and processes across academic and industrial applications. In this work, coupled phenomena and multiphysics was utilized, including the diffusion transport of O₂ in PDMS and water, transport by advective flow, and boundary conditions such as O₂ sources and sinks, to numerically simulate O₂ transport.

By reconstructing the 3D geometries, defining material properties, and setting boundary conditions, numeric models can be built to verify and confirm experimental results, as well as to perform complex in silico analyses that would otherwise require significant experimental efforts. In **Paper I**, the 3D geometries of the PDMS device were simulated using COMSOL Multiphysics (version 5.1) to verify the experimental results obtained with sensPIV particles under both flow and no-flow conditions in the PDMS device. By comparing the experimental measurements with the numerically simulated results, the reliability of sensPIV was assured.

Chapter 3: Applications of Microscale O₂ Measurements and Findings

Last chapter introduced the principle and techniques for O₂ measurement at microscales. This chapter summarizes these developed methodologies aimed at measuring O₂ dynamics in microenvironments and cellular O₂ respiration under tuneable chemical conditions. The goal of these techniques is to enhance our understanding of how O₂ dynamics influence the responses of individual organisms and how to use O₂ as a proxy for metabolism in toxicological studies. This chapter will introduce the model organisms used in this PhD thesis - marine corals, diatoms, and human hepatic cells - and highlight key findings from the investigations into their O₂ metabolism and responses to environmental changes.

SensPIV: tracking O₂ fluxes at the microscale

In **Paper I**, my contribution involved fabricating a three-channel PDMS microfluidic device, which enables the precise control and observation of O₂ dynamics. The PDMS device was used to validate and demonstrate the ability of sensPIV particles to simultaneously visualize fluid flow and O₂ concentrations in well-controlled O₂ environments. The successful tracking of O₂ gradients and laminar flow fields within the PDMS device produced results consistent with the simulation model that I created using COMSOL Multiphysics v5.1. In this model, the PDMS channel structures were recreated, and the flow fields and O₂ gradients in the middle channel were modelled. The comparison between experimental results and numerical model proved that sensPIV is a reliable tool for measuring and visualizing O₂ dynamic transport at microscales.

Paper I also describes the application of sensPIV, implemented by Ahmerkamp Lab in Max Planck Institute, to measure the O₂ dynamics on the surface of the coral species *Porites lutea*. This revealed how coral cilia movements change in response to dynamic changes in O₂ gradients. By visualizing O₂ concentrations and flow fields with optode microparticles, it was discovered that upward fluid movement driven by cilia corresponded with areas of higher O₂ concentration, while downward flows matched areas of lower O₂ concen-

tration. This challenges the previous belief that cilia uniformly mix the boundary layer, instead indicating that cilia adjust their movements to improve the upward transport of excess O_2 from coral tissue. Additionally, O_2 was directed downward towards the mouth openings, where respiration occurs, linking O_2 production and consumption areas to potentially speed up metabolism. This finding emphasizes the ecological role of cilia-induced advection and provide an in-depth understanding of O_2 mass transport mechanisms in coral physiology.

Micro-respiration chamber: size-related respiration kinetics of single hepatic cells

In **Paper II**, a micro-respiration chamber for measuring single-cell O_2 respiration in mammalian HepG2 cells was fabricated. The closed microwells with O_2 -sensitive optodes planar decoration at the well bottom generate an array of gas-tight chambers where single-cells were immobilized, and their cellular OCR were measured. HepG2 cells were firstly measured in the device because they are popular as an *in vitro* model and broadly used for studying liver physiology, drug metabolism, and toxicology, as they maintain various liver-specific functions, including drug and xenobiotic metabolism, protein synthesis, and lipid metabolism regulation¹⁴⁰.

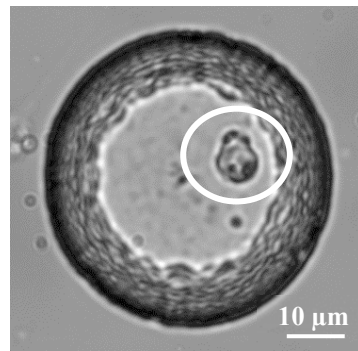


Figure 11. A single HepG2 cell isolated in a glass microwell. The diameter of the microwell is 50 μm , and the microwell depth is 20 μm .

The O_2 respiration rate of single HepG2 cells was determined using the micro-respiration chamber and the resulting data was analyzed through a multiparameter identification algorithm developed by Ahluwalia Lab at Pisa University. The results revealed that individual cells have an O_2 -dependent metabolic rate that follows Michaelis-Menten kinetics, with maximal O_2 consumption rates significantly lower than those observed in cell monolayers or 3D aggregates. Additionally, the presence of multiple cells (ranging from 2 to 7) within the same microwell reduced the maximal single-cell consumption rate, indicating an adaptive response to limited O_2 availability.

By examining the covariance of cell size and O_2 consumption within the population of HepG2 cells, the study demonstrated that cooperative behavior

emerges among multiple cells and that single-cell metabolism can be described by a lognormal joint probability density. This detailed characterization of cellular metabolism provides a foundational understanding that is crucial for designing therapeutic strategies and tissue engineering applications. It underscores the importance of considering cellular interactions in metabolic studies, as these interactions can significantly influence cellular behavior and metabolic rates.

SlipO₂Chip: O₂ metabolic changes of diatom single-cells under HHQ treatments

In **Paper III**, I developed a microfluidic platform called SlipO₂Chip to characterize the respiration of single diatom cells before and after various levels of HHQ treatments. SlipO₂Chip combined the principles of SlipChip, a microfluidic device that facilitated the introduction and exchange of liquids in microwells through slipping motions of a channel, with the micro-respiration chamber device described in **Paper II** for single-cell O₂ respiration measurements. In the SlipO₂Chip platform, optode-decorated microwells containing single diatom cells were designed to be opened or closed through the slipping motion of the channel. When the channel overlapped with the microwells, it allowed for the exposure of diatom cells to different concentrations of HHQ. By slipping the channel away, the microwells can be sealed for precise O₂ respiration measurements.

The diatom species studied within SlipO₂Chip was *Ditylum brightwellii* (Figure 12), which ranges in size from 50 to 120 μm in length and 10 to 40 μm in width. Diatoms were selected as a model species because they dominate phytoplankton communities²⁹⁻³¹ and are unicellular microalgae.

SlipO₂Chip allowed for the precise quantification of single-cell O₂ respiration and enabled us to examine the effects of the bacterial quorum sensing molecule HHQ on diatom cellular O₂ respiration. The results showed a dose-dependent decrease in O₂ respiration rates, with a maximum reduction of 40.2% observed at HHQ concentrations exceeding 35.5 μM and an EC₅₀ of 5.8 μM. These single-cell measurements were consistent with bulk respiration methods but provided insights into cell-to-cell variability, underscoring the importance of SlipO₂Chip measurements in ecotoxicological applications. These insights are vital for developing strategies to mitigate the impacts of environmental stressors on these critical primary producers and their associated ecosystems.

Combining micro-respiration chamber with QPI: incorporating bio-variability into metabolic scaling theory

In **Paper IV**, the micro-respiration chamber device was integrated with the optical QPI system for the combined measurement of O₂ respiration and dry mass of same single-cells.

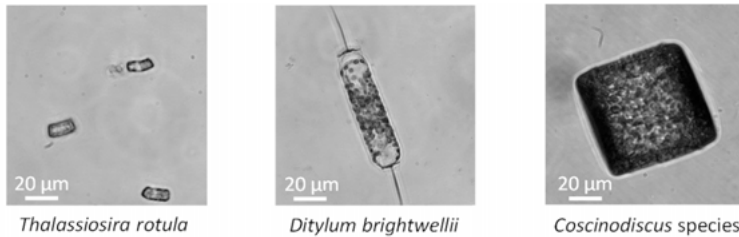


Figure 12. The three model diatom species used in experiments: *Thalassiosira rotula* (16 - 24 µm), *Ditylum brightwellii* (50 - 120 µm), and *Coscinodiscus* species (200 - 300 µm).

Three diatom species *Thalassiosira rotula*, *Ditylum brightwellii*, *Thalassiosira rotula*, and *Coscinodiscus* species in a wide range of cell sizes, spanning from 16 µm to 300 µm (Figure 12) were chosen as model organisms to investigate the allometric scaling between cellular O₂ respiration rates and dry mass. Experiments also benefited from these species' rapid growth rates¹⁴¹.

Collected data was fitted to a power Law of the form $R = aM^b$, describing how diatom cells' O₂ consumption rate is allometrically scaled with their dry mass. For interspecies scaling, the scaling exponent b values for *Thalassiosira rotula*, *Ditylum brightwellii*, *Thalassiosira rotula*, and *Coscinodiscus* species were 0.19, 0.43 and 0.12 respectively. The intraspecies scaling power constant across the three species was 0.78, which was close to the widely used reference value 3/4. These findings, in some degrees, proved the feasibility of including the joint measurement data into scaling theory frameworks. The cellular measurements also potentially completed the scaling pattern at the single-cell level, helping us understand how this cellular bio-variability would alter the scaling model.

However, the herein used QPI system introduced uncertainty in dry mass values, necessitating future calibration for accuracy. One of the uncertainties technically raised from the roughness of microwell bottom. And the other problem to be solved is how to exactly measure diatoms, should the silica shell, known as frustule, be included or not. Although the diatom frustule does not directly participate in cell metabolism, excluding it from measurements

could underestimate the cell's total dry mass, which is crucial given its role in buoyancy, protection, and overall cellular function¹⁴². But overall, these results highlight the importance of considering both interspecies and intraspecies variations in metabolic studies, with significant implications for enhancing the precision of current scaling theory framework by adding cell-to-cell heterogeneity.

Chapter 4: Concluding Remarks and Future Perspectives

In this PhD thesis, a series of microfluidic and LoC systems were developed, capable of tracking O₂ dynamics using optode microparticles, or maintaining single-cells in planar optode-decorated micro-chambers for intracellular O₂ respiration measurement under controlled chemical environments. These innovative applications of O₂-sensitive optodes in microfluidic and LoC setups exemplified the integration of advanced sensing technologies in microchambers, providing foundational tools for ecological and toxicological research.

Paper I introduces the sensPIV technique and demonstrates that PtTFPP optode micro-particles can effectively track the spatiotemporal dynamics of biological O₂ metabolism in aquatic environments. Beyond its contributions to understanding O₂ mass-transfer processes at the microscale, sensPIV holds potential for measuring multiple chemical dynamics. Isolating the effects of O₂ dynamics from these interacting factors makes it challenging to attribute many observed ecological effects solely to O₂ availability¹⁴³. For example, many studies have found that hypoxia inhibits the growth of diatoms^{47,48}, but the combination of hypoxia with elevated CO₂ levels can alter this outcome - enhancing diatom growth and phytoplankton productivity despite reduced O₂ availability¹⁴⁴. Developing optode microparticles capable of sensing pH, CO₂, H₂S, and NH₃³⁴ would significantly enhance our ability to investigate complex biological processes in aquatic systems.

Papers II-IV introduce glass LoC devices that allow for single-cell O₂ metabolism measurements. **Paper II** provides foundational insights into the size-related metabolic variability of single human hepatic cells and their adaptation to local O₂ availability. By employing the high-throughput microfabricated devices, the study elucidates the scaling laws connecting single-cell metabolism to tissue-level functions¹⁴⁵, informing more accurate models of liver metabolism and better therapeutic strategies. The observed cooperative behavior in cell clusters underscores the importance of considering cellular interactions in metabolic studies, potentially leading to more effective liver disease treatments.

Paper III presents SlipO₂Chip, a core pillar of this thesis. SlipO₂Chip assessed the impact of the bacterial secondary metabolite HHQ on single diatom cells' O₂ consumption, showcasing its potential for advancing toxicology and pharmacology research. Measuring respiration before and after chemical exposure provides a clearer understanding of cellular heterogeneity and its impact on metabolic responses. This capability is particularly beneficial in applications such as clinical biopsies and studies involving rare microbial isolates, where sample volumes are limited. The findings highlight the importance of single-cell analysis in detecting chemically tolerant subpopulations, potentially leading to more targeted and effective interventions in environmental and medical contexts. Future work may involve characterizing the O₂ metabolism of individual phytoplankton cells under different levels of naturally occurring pollutants, such as herbicides and heavy metals.

Meanwhile, the superior optical properties of the glass micro-respiration chamber system allow for coupling with other optical analysis methods, such as QPI, as described in **Paper IV**, for cellular dry mass measurement. This combination resulted in a high-throughput toxicological screening platform simultaneously captures information about cellular mass and metabolism on a per-cell basis. This method scales metabolic measurements across various cell types and significantly enhances study accuracy by enabling the direct observation of individual cellular responses.

The methodologies developed in this thesis enable a deeper understanding of organism-O₂ fluxes interactions in microenvironments as well as single-cell O₂ respiration quantifications, highlighting the importance of microscale O₂ measurement in scientific models.

Lastly, the research presented in this thesis adheres to ethical standards and guidelines for conducting experiments involving living organisms. The methodologies were designed to use less biological material and chemical reagents.

Chapter 5: Summary of the Included Papers

Paper I: Simultaneous visualization of flow fields and O₂ concentrations to unravel transport and metabolic processes in biological systems

This paper presents a method called sensPIV, which utilized chemically sensing microparticles to simultaneously measure O₂ concentrations and flow fields within and around biological systems. This method offered a simple yet powerful tool for visualizing the interactions between physical transport processes and biological metabolisms in various life-science and engineering applications.

The sensPIV technique provides insights into the O₂ dynamics by tracking O₂-sensitive microparticles with imaging technologies, enabling real-time monitoring and instant referencing of changes in O₂ concentrations. For instance, in corals, sensPIV demonstrated how ciliary movements optimize metabolic processes by modifying local O₂ concentrations. This method surpassed traditional approaches by allowing simultaneous, real-time visualization of both O₂ distributions and fluid movements across different spatial scales and environments, providing a comprehensive understanding of the complex interactions within biological systems. The results underlined the potential of sensPIV in extending to various research fields, particularly where understanding the microscale interactions of flow and biological reactions is crucial.

Paper II: Size-related variability of O₂ consumption rates in individual human hepatic cells

The paper introduces a novel microfabricated device to investigate single-cell O₂ consumption rates in human hepatic cells. The device employed microwells coated with a luminescent O₂-sensitive optode material, allowing precise measurement of O₂ consumptions at the individual cell level. This enabled observations of Michaelis-Menten kinetics in O₂ metabolism, which are usually masked in traditional monolayer or aggregate cell cultures.

The study revealed that individual cells and several (2 - 7) cells adjust their maximum O₂ consumption rates based on the local O₂ availability, a phenomenon that highlighted the adaptability of cells to their microenvironment. Such findings could not be detected through traditional bulk cell studies, thus underscoring the importance of single-cell analysis. The paper also described a multiparameter identification algorithm used to correlate cell size with O₂ consumption rates, offering new insights into the metabolic behaviour of cells.

Additionally, a lognormal distribution was found in the joint probability density of cell size and metabolism rates, suggesting that size and metabolic rate are intrinsically linked in a predictable manner. This relationship is critical for understanding how cells adapt to environmental changes and could improve the design of biomedical and biotechnological applications such as drug testing and cell-based therapies.

Overall, the study provided a robust framework for exploring the metabolic dynamics of single-cells and their implications for tissue and organ level functions.

Paper III: SlipO₂Chip- single-cell respiration under tuneable environments

This manuscript introduces SlipO₂Chip, an innovative glass microfluidic device designed to measure single-cell O₂ metabolism under tuneable chemical perturbations. Inspired by the original SlipChip⁴⁰, which facilitated multiplexed microfluidic reactions, SlipO₂Chip enhanced functionality for single-cell studies by enabling precise controls of the chemical microenvironment, and repeated O₂ respiration measurement on the same cells before and after chemical treatments.

SlipO₂Chip featured two main components: a bottom microwell plate and a top channel plate, both made of glass. The bottom plate contained microwells coated with O₂-sensitive optodes. This setup allowed precise control of the fluid environment surrounding the cells, enabled by the slipping movement of the top plate, which can either expose the cells to different chemical solutions or seal them off for analysis of their respiration.

A critical innovation of SlipO₂Chip is its ability to perform sequential measurements of single-cell respiration before and after exposure to chemical solutes on the same cells. This is demonstrated by measuring the effects of the bacterial signal molecule HHQ on the dark respiration of diatoms, revealing dose-dependent effects consistent with conventional bulk measurements.

SlipO₂Chip allows for repeated, non-invasive, and time-resolved measurements, making it suitable for applications with limited sample volumes, such as clinical biopsies or rare microbial isolates.

Paper IV: Combined measurements of single-cell oxygen metabolism and dry mass

This manuscript describes the application of the glass micro-respiration chamber device designed for the simultaneous measurement of single-cell O₂ respiration rates and cellular dry mass in three diatom species of varying sizes. The device integrated O₂-sensitive optodes into microwells, which immobilized single diatom cells for O₂ respiration measurement. Its superior optical properties allowed for the use of QPI, a non-invasive microscopy technique that measures cell dry mass by analyzing light retardation.

Initial measurements yielded combined data on dry mass and respiration rate on same cells for three diatom species: *Thalassiosira rotula*, *Ditylum brightwellii*, and *Coscinodiscus* species, with cell sizes ranging from 16 to 300 µm. The study examines how cellular bio-variability influences the scaling framework. Results revealed distinct interspecific and intraspecific metabolic scaling patterns. *Thalassiosira rotula* and *Coscinodiscus* species displayed smaller scaling exponents compared to *Ditylum brightwellii*. This underscored the impact of morphological and physiological traits of diatom cells on their metabolic efficiency and signified the importance of including cell-to-cell heterogeneity in the scaling theory. Meanwhile, the interspecific exponent across three species closely aligned with the 3/4 power law, supporting the general metabolic scaling theory.

Challenges such as microwell roughness affecting QPI accuracy and the inclusion of diatom frustules in dry mass calculations emphasize the complexity of precise measurement. The need for rigorous calibration using standard beads and methodological refinement, such as cell segmentation, is highlighted. Future plans involve using 2-photon printing to fabricate smoother microwells, thereby reducing measurement inaccuracies due to surface roughness.

Integrating respiration and dry mass measurements at the single-cell level serves as a crucial proof of concept, demonstrating the feasibility and importance of this approach in studying metabolic scaling with cellular variability.

Popular Science Summary

This thesis delves into innovative microfluidic and Lab-on-a-Chip (LoC) technologies, tools that downscale the world, to enhance our understanding of oxygen (O_2) dynamics at the microscale and their relationship with biological processes. These advanced devices, coupled with optical O_2 sensors, enable precise, real-time visualization of O_2 dynamics in aquatic environments and cellular respiration under various chemical conditions. By capturing and processing this information, these technologies reveal the micro-world, demonstrating how organisms and microorganisms like corals, mammalian cells, and diatoms breathe and respond to environmental changes such as pollutant exposure and warming, shedding light on their adaptive behaviors.

One major breakthrough is the development of sensPIV. This technique uses O_2 -sensitive microparticles to simultaneously measure O_2 concentrations and fluid flow within biological systems. By embedding these microparticles in the environment, sensPIV tracks real-time changes, providing a dynamic view of how physical transport processes interact with biological metabolism. For example, in coral ecosystems, sensPIV has demonstrated how ciliary movements optimize metabolic processes by adjusting local O_2 levels. This method offers a more comprehensive understanding than traditional approaches by visualizing O_2 distribution and fluid movements concurrently, opening new possibilities for studying ecological and physiological processes in unprecedented detail.

Another study introduces an optode planar-decorated micro-respiration chamber device for measuring mammalian single-cell O_2 consumption rates. Traditional bulk cell culture methods often mask individual variations and behaviors. This new device overcomes such limitations by using encapsulated microwells coated with O_2 -sensitive planar optodes, allowing precise measurements of cellular O_2 metabolism. The study reveals that individual cells adjust their O_2 consumption based on local availability, highlighting previously hidden adaptability. Understanding these individual behaviors is crucial for biomedical research applications, such as drug testing and cell-based therapies, where individual cell responses can significantly impact overall outcomes. Additionally, this work employs a multiparameter identification algorithm to

correlate cell size with O₂ consumption rates, offering new insights into cellular metabolic behavior. The observed lognormal distribution in the joint probability density of cell size and metabolic rates suggests a predictable relationship, providing a new perspective for future research.

The SlipO₂Chip represents another significant advancement. This sophisticated glass microfluidic device is designed to measure single-cell O₂ metabolism in diatoms under varying chemical conditions. Inspired by the original SlipChip, SlipO₂Chip simplifies the manipulation of individual cells, allows precise control of the microenvironment, and facilitates repeated measurements of O₂ respiration before and after chemical exposure. Comprising a microwell plate with O₂-sensitive optodes and a movable channel plate, the device can alternately expose or seal cells for respiration analysis. This capability was demonstrated by examining the effects of the bacterial signal molecule HHQ on diatom respiration, revealing dose-dependent responses consistent with conventional bulk measurements. SlipO₂Chip's design, enabling non-invasive, repeated measurements, is particularly beneficial for applications with limited sample volumes, such as clinical biopsies or rare microbial isolates. This technology significantly enhances research in cellular biology, toxicology, and pharmacology by providing detailed insights into cellular responses to environmental and chemical changes.

The integration of O₂-sensitive sensors with Quantitative Phase Imaging (QPI) in a glass micro-respiration chamber device marks another important development. This device allows for simultaneous measurement of single-cell O₂ metabolism and dry mass, providing a comprehensive view of cell function. QPI is a non-invasive microscopy technique that calculates cell dry mass by measuring how light is slowed as it passes through the cell. By combining O₂-sensitive optodes and QPI, researchers can gather detailed data on both the metabolic and physical properties of cells. Initial experiments showcased the device's capacity to simultaneously measure dry mass and metabolism across different diatom species. This information can be incorporated into established scaling frameworks, like Kleiber's law, to improve predictions of microbial community responses to environmental changes.

Collectively, this thesis demonstrates the transformative potential of integrating O₂ optodes with LoC tools for tracking O₂ dynamics at the microscale and conducting advanced single-cell analyses. These innovations enable more precise and comprehensive studies of cellular metabolism, promising improvements in medical treatments and environmental interventions. Understanding cellular responses to their microenvironment at an individual level provides deeper insights into cellular heterogeneity, paving the way for more targeted and effective therapeutic strategies. This research advances our knowledge of

cellular behavior and interactions with the environment, setting the stage for future breakthroughs in biological, toxicological, and medical fields.

Populärvetenskaplig sammanfattning

Denna avhandling utforskar innovativa mikrofluidiska och Lab-on-a-Chip (LoC) teknologier, verktyg som förminskar världen, för att förbättra vår förståelse av syredynamik (O_2) på mikroskalan och dess förhållande till biologiska processer. Dessa avancerade enheter, kombinerade med optiska O_2 -sensors, möjliggör exakt, realtidsvisualisering av O_2 -dynamik i vattenmiljöer och cellandning under olika kemiska förhållanden. Genom att fånga och bearbeta denna information avslöjar dessa teknologier mikrovärlden och visar hur marina organismer och mikroorganismer som koraller och diatomer andas och reagerar på miljöförändringar såsom föroreningsexponering och uppvärmning, vilket belyser deras anpassningsbeteenden.

Ett stort genombrott är utvecklingen av Chemical Sensing Particle Image Velocimetry (sensPIV). Denna teknik använder O_2 -känsliga mikropartiklar för att samtidigt mäta O_2 -koncentrationer och vätskeflöden inom biologiska system. Genom att integrera dessa mikropartiklar i miljön spårar sensPIV förändringar i realtid och ger en dynamisk bild av hur fysiska transportprocesser interagerar med biologisk metabolism. Till exempel, i korallekosystem, har sensPIV visat hur cilierörelser optimerar metaboliska processer genom att justera lokala O_2 -nivåer. Denna metod erbjuder en mer omfattande förståelse än traditionella metoder genom att samtidigt visualisera O_2 -fördelning och vätskeflöden, vilket öppnar nya möjligheter för att studera ekologiska och fysiologiska processer i en enastående detalj.

En annan studie introducerar en optode-planar-dekorerad mikro-respirationskammarenhet för att mäta O_2 -förbrukningshastigheter i enskilda däggdjursceller. Traditionella bulkcellodlingsmetoder döljer ofta individuella variationer och beteenden. Denna nya enhet övervinner sådana begränsningar genom att använda placera cellerna i mikrobrunnar som är belagda med O_2 -känsliga plana optoder, vilket möjliggör precisa mätningar av cellulär O_2 -metabolism. Studien avslöjar att individuella celler justerar sin O_2 -förbrukning baserat på lokal tillgänglighet, vilket belyser tidigare dolda anpassningsförmågor. Förståelsen av dessa individuella beteenden är avgörande för biomedicinska forskningsapplikationer, såsom läkemedelstestning och cellbaserade terapier, där individuella cellresponser kan ha betydande inverkan på

övergripande resultat. Dessutom använder detta arbete en multiparameteridentifieringsalgoritm för att korrelera cellstorlek med O₂-förbrukningshastigheter, vilket erbjuder nya insikter i cellulärt metabolisk beteende. Den observerade lognormala fördelningen i den gemensamma sannolikhetstätheten av cellstorlek och metaboliska hastigheter tyder på ett förutsägbart förhållande, vilket ger ett nytt perspektiv för framtida forskning.

SlipO₂Chip representerar ytterligare ett betydande framsteg. Denna sofistikerade glasmikrofluidiska enhet är designad för att mäta enkelcellig O₂-metabolism i diatomer under varierande kemiska förhållanden. Inspirerad av den ursprungliga SlipChip, förenklar SlipO₂Chip manipulationen av individuella celler, möjliggör exakt kontroll av mikromiljön och underlättar upprepade mätningar av O₂-respiration före och efter kemisk exponering. Bestående av en mikrobägarplatta med O₂-känsliga optoder och en rörlig kanalplatta, kan enheten växelvis exponera eller försegla celler för respirationsanalys. Denna förmåga demonstrerades genom att undersöka effekterna av den bakteriella signalmolekylen HHQ på diatomrespiration, vilket avslöjade dosberoende responser som är förenliga med konventionella bulkmätningar. SlipO₂Chips design, som möjliggör icke-invasiva, upprepade mätningar, är särskilt fördelaktig för applikationer med begränsade provvolym, såsom kliniska biopsier eller sällsynta mikrobiella isolat. Denna teknologi förbättrar forskningen inom cellbiologi, toxikologi och farmakologi genom att tillhandahålla detaljerade insikter i cellresponser på miljö- och kemiska förändringar.

Integrationen av O₂-känsliga sensorer med Quantitative Phase Imaging (QPI) i en glasmikro-respirationskammarenhet markerar ytterligare en viktig utveckling. Denna enhet möjliggör samtidig mätning av enkelcellig O₂-metabolism och torr massa, vilket ger en omfattande bild av cellfunktion. QPI är en icke-invasiv mikroskopiteknik som beräknar cellens torrmasa genom att mäta hur ljus bromsas när det passerar genom cellen. Genom att kombinera O₂-känsliga optoder och QPI kan forskare samla detaljerade data om både de metaboliska och fysiska egenskaperna hos celler. Inledande experiment visade enhetens kapacitet att samtidigt mäta torrmasa och metabolism av olika diatomarter. Denna information kan integreras i etablerade skalningsramverk, som Kleibers lag, för att förbättra förutsägelser av mikrobiella populationers svar på miljöförändringar.

Sammanfattningsvis visar denna avhandling den transformativa potentialen av att integrera O₂-optoder med LoC-verktyg för att spåra O₂-dynamik på mikroskalan och utföra avancerade analyser på enskilda celler. Dessa innovationer möjliggör mer precisa och omfattande studier av cellulär metabolism, vilket lovar förbättringar i medicinska behandlingar och miljöinterventioner. Att förstå cellresponser på deras mikromiljö på individuell nivå ger djupare insikter i cellulär heterogenitet, vilket banar väg för mer målinriktade och effektiva

terapeutiska strategier. Denna forskning fördjupar vår kunskap om cellbete-
ende och interaktioner med miljön, vilket lägger grunden för framtida genom-
brott inom biologiska, toxikologiska och medicinska områden.

Acknowledgements

In the journey that has been the creation of this thesis, I was accompanied by the indelible presence of those who imparted wisdom, shared in efforts, and celebrated the small victories that lined the path to this culmination. This thesis is not merely a reflection of my own work, but a mosaic of the contributions and encouragements of many.

First and foremost, I wish to express my gratitude to my supervisor, **Lars**. Your support and guidance as my Master and PhD supervisor over the past five years have been invaluable. I feel exceptionally fortunate to have participated in your projects, which has provided an unparalleled learning experience. Reflecting on our shared journey, it is profoundly moving to see how far we have pushed forward. I appreciate your unwavering enthusiasm for academia, which keeps reminding me of my initial aspirations and will remain a big motivation for me in the future.

I would like to convey my sincere gratitude to my co-supervisor, **Maria Tenje**, for your invaluable mentoring and guidance in microfluidics, as well as the information and encouragement you provided. My heartfelt thanks to my co-supervisor **Klaus** for your insightful contributions to oxygen sensing. I am also deeply grateful to my co-supervisor **Joëlle** for the indispensable administrative support throughout my PhD study.

I would like to thank all collaborators for their hard work and active engagements. Thank you, **Milena** for all your teaching and tutoring at Myfab and for your consistent assistance in tackling technical problems at any time. I would also like to express my appreciation to the **Stocker Lab**, **Ahluwalia Lab**, and **Rinaldo Lab** from the **Sinergia program**. Thank you, **Ermes**, for the exciting lab work and discussions that we've had together. Thank you, **Oliver** and **Dieter**, though remotely, sharing the PhD journey with you has made it much more enjoyable and rewarding. Thank you, **Johannes**, **Clara**, and **Francesco**, for the enriching monthly catch-up meetings - communicating with you has provided precious opportunities to broaden my perspectives and seek advice. Also, I am thankful to **Roberto**, **Eleonora**, **Ela**, **Uria** for your support during my master thesis. To **Laurent**, thank you for your intricate ideas and brain-

storming sessions. To **Atena** and **Sofia**, thank you for teaching me microfabrication techniques. And thank **Sven**, **Örjan**, **Rimantas**, **Ernesto** and **Tomas** for the training and technical assistance in the cleanroom.

I would like to thank my colleagues from the **Behrendt Lab** - **Linhong**, **Saskia**, **Xavi**, **Olle**, **Jeanne**, **Michael**, and all the master and internship students. Thank you for the engaging conversations and the countless amusing moments in the lab and office. I would like to extend my thanks to **Andrea**, **Manolis**, **Polina**, **Sofie**, **Michela**, **Fatih**, **Farnaz**, **Violeta**, **Caroline**, **John**, **Diana**, **Fábio**, **Adeolu**, **Marie**, **Maria Jönsson**, **Sonja**, **Dimitris**, **Carlos** - all the previous and current **PhET** members for together fostering a pleasing and warm work environment. I would also like to thank colleagues from the **EM-BLA Lab**, **MST**, and **BME** divisions for your valuable input and assistance - **Susan**, **Sarah**, **Abdul**, **Gabriel**, **Federico**, **Ana Maria**, **Samah**, **Neeraj**, **Sagar**, **Jan**, **Bei**, and **Lena**.

Special thanks to my friends **Dodo**, **Xiaofang**, and **Yingying**. I am fortunate to have grown up with you and to continue sharing your company. Thank you, **Ela**, and your families, for all the care and cherished moments. Thank you, **Jihyun**, **Kang**, **Shiyu**, **Yixi**, **Tianyu**, and **Jingyi**. Life continuously moves forward, and I am elated that each stage bears traces of you. Thank you, **Qian**, for all the memorable chats and experiences in Uppsala. Thank you, **Zhenhua**, for your prayers for my defense - you are the best Shixiong. Thank you, **Jing**, for sharing your talents in mushroom, movies and sports. Thank you, **Zhouyuan** and **Hongyu**, for the sth time and opinion sharing. Thank you **Xueying**, **Pei**, **Dafu**, **Linglu** and **Huasi**, for the happy moments. And thank you to the board game hosts and buddies - **Zheqiang**, **ChenCheng**, **Yuan Zhu**, **Yingtao**, and **Zhuzhu**.

Last, but not least, to **my parents**, whose love have been the silent yet steadfast foundation of all my journeys. **爸爸妈妈**, 成为你们的孩子是我最大的幸运和骄傲。你们赋予了我身上最积极的部分，这些部分和你们的包容与信任就像一个巨大的泡泡包裹着我，给我安全感，载我去任何想去的地方。正是在这些旅程中的某一刻，我终于觉得自己也变成了大人。一般来说，没有比大人更大的人了，但你们仍然一直在我身后。谢谢你们，爱你们。

For the strength imparted to me by each of you, I am sincerely grateful. May this thesis not only signify an end but also the beckoning of new beginnings. With all my heart, thank you.

Yuan
August 2024

Bibliography

1. Houghton, J. Global warming. *Reports on Progress in Physics* **68**, 1343–1403 (2005).
2. Cheng, L. *et al.* Past and future ocean warming. *Nat Rev Earth Environ* **3**, 776–794 (2022).
3. Häder, D.-P. *et al.* Anthropogenic pollution of aquatic ecosystems: Emerging problems with global implications. *Science of The Total Environment* **713**, 136586 (2020).
4. Palombo, M. R. Thinking about the Biodiversity Loss in This Changing World. *Geosciences (Basel)* **11**, 370 (2021).
5. Cottingham, K. L., Brown, B. L. & Lennon, J. T. Biodiversity may regulate the temporal variability of ecological systems. *Ecol Lett* **4**, 72–85 (2001).
6. Hautier, Y. *et al.* Anthropogenic environmental changes affect ecosystem stability via biodiversity. *Science (1979)* **348**, 336–340 (2015).
7. Valiente-Banuet, A. *et al.* Beyond species loss: the extinction of ecological interactions in a changing world. *Funct Ecol* **29**, 299–307 (2015).
8. Stryer, L., Tymoczko, J. L. & Berg, J. M. Biochemistry 5th ed Freeman. *WH and Company* **41**, (2002).
9. Van Valen, L. Evolution as a zero-sum game for energy. *Evolutionary Theory* **4**, 289–300 (1980).
10. Brown, J. H., Gillooly, J. F., Allen, A. P., Savage, V. M. & West, G. B. Toward a metabolic theory of ecology. *Ecology* **85**, 1771–1789 (2004).
11. Glazier, D. S. Is metabolic rate a universal ‘pacemaker’ for biological processes? *Biological Reviews* **90**, 377–407 (2015).
12. Brown, J. H., Burger, J. R., Hou, C. & Hall, C. A. S. The pace of life: metabolic energy, biological time, and life history. *Integr Comp Biol* **62**, 1479–1491 (2022).
13. Cheung, W. W. L., Wei, C.-L. & Levin, L. A. Vulnerability of exploited deep-sea demersal species to ocean warming, deoxygenation, and acidification. *Environ Biol Fishes* **105**, 1301–1315 (2022).
14. Dominović, I. *et al.* Deoxygenation and stratification dynamics in a coastal marine lake. *Estuar Coast Shelf Sci* **291**, 108420 (2023).

15. Popova, E. *et al.* From global to regional and back again: common climate stressors of marine ecosystems relevant for adaptation across five ocean warming hotspots. *Glob Chang Biol* **22**, 2038–2053 (2016).
16. Ross, T., Du Preez, C. & Ianson, D. Rapid deep ocean deoxygenation and acidification threaten life on Northeast Pacific seamounts. *Glob Chang Biol* **26**, 6424–6444 (2020).
17. Schramski, J. R., Dell, A. I., Grady, J. M., Sibly, R. M. & Brown, J. H. Metabolic theory predicts whole-ecosystem properties. *Proceedings of the National Academy of Sciences* **112**, 2617–2622 (2015).
18. Nisbet, R. M., Ross, A. H. & Brooks, A. J. Empirically-based dynamic energy budget models: theory and an application to ecotoxicology. *Nonlinear World* **3**, 85–106 (1996).
19. Nisbet, R. M., Muller, E. B., Lika, K. & Kooijman, S. From molecules to ecosystems through dynamic energy budget models. *Journal of animal ecology* 913–926 (2000).
20. Atkinson, D. & Sibly, R. M. Why are organisms usually bigger in colder environments? Making sense of a life history puzzle. *Trends Ecol Evol* **12**, 235–239 (1997).
21. Angilletta, Jr. , , M. J. & Dunham, A. E. The temperature-size rule in ectotherms: simple evolutionary explanations may not be general. *Am Nat* **162**, 332–342 (2003).
22. Kleiber, M. Body size and metabolism. *Hilgardia* **6**, 315–353 (1932).
23. Feldman, H. A. & McMahon, T. A. The mass exponent for energy metabolism is not a statistical artifact. *Respir Physiol* **52**, 149–163 (1983).
24. Savage, V. M. *et al.* The predominance of quarter-power scaling in biology. *Funct Ecol* **18**, 257–282 (2004).
25. Glazier, D. S. Beyond the ‘3/4-power law’: variation in the intra- and interspecific scaling of metabolic rate in animals. *Biological Reviews* **80**, 611–662 (2005).
26. Alcaraz, M. Marine zooplankton and the metabolic theory of ecology: Is it a predictive tool? *J Plankton Res* **38**, 762–770 (2016).
27. Brierley, A. S. & Kingsford, M. J. Impacts of climate change on marine organisms and ecosystems. *Current Biology* **19**, R602–R614 (2009).
28. Behrenfeld, M. J. *et al.* Biospheric primary production during an ENSO transition. *Science (1979)* **291**, 2594–2597 (2001).
29. Basu, S. & Mackey, K. Phytoplankton as key mediators of the biological carbon pump: Their responses to a changing climate. *Sustainability* **10**, 869 (2018).
30. Alvain, S., Moulin, C., Dandonneau, Y. & Loisel, H. Seasonal distribution and succession of dominant phytoplankton groups in the global ocean: A satellite view. *Global Biogeochem Cycles* **22**, (2008).
31. Tréguer, P. *et al.* Influence of diatom diversity on the ocean biological carbon pump. *Nat Geosci* **11**, 27–37 (2018).

32. Etzkorn, J. R. *et al.* Using micro-patterned sensors and cell self-assembly for measuring the oxygen consumption rate of single cells. *Journal of Micromechanics and Microengineering* **20**, 95017 (2010).
33. Molter, T. W. *et al.* A microwell array device capable of measuring single-cell oxygen consumption rates. *Sens Actuators B Chem* **135**, 678–686 (2009).
34. Koren, K. & Zieger, S. E. Optode based chemical imaging—possibilities, challenges, and new avenues in multidimensional optical sensing. *ACS Sens* **6**, 1671–1680 (2021).
35. Quaranta, M., Borisov, S. M. & Klimant, I. Indicators for optical oxygen sensors. *Bioanalytical Reviews* vol. 4 115–157 Preprint at <https://doi.org/10.1007/s12566-012-0032-y> (2012).
36. Kelbauskas, L. *et al.* A platform for high-throughput bioenergy production phenotype characterization in single cells. *Sci Rep* **7**, 45399 (2017).
37. Hu, C. & Popescu, G. Quantitative Phase Imaging: Principles and Applications. in *Label-Free Super-Resolution Microscopy* 1–24 (2019). doi:10.1007/978-3-030-21722-8_1.
38. Cao, Q., Yu, J. & Connell, D. New allometric scaling relationships and applications for dose and toxicity extrapolation. *Int J Toxicol* **33**, 482–489 (2014).
39. Sharma, V. & McNeill, J. H. To scale or not to scale: the principles of dose extrapolation. *Br J Pharmacol* **157**, 907–921 (2009).
40. Du, W., Li, L., Nichols, K. P. & Ismagilov, R. F. SlipChip. *Lab Chip* **9**, 2286 (2009).
41. Reen, F. J. *et al.* The Pseudomonas quinolone signal (PQS), and its precursor HHQ, modulate interspecies and interkingdom behaviour. *FEMS Microbiol Ecol* **77**, 413–428 (2011).
42. Del Giorgio, P. & Williams, P. *Respiration in Aquatic Ecosystems*. (OUP Oxford, 2005).
43. Storey, K. B. & Storey, J. M. Oxygen limitation and metabolic rate depression. *Functional metabolism: regulation and adaptation* 415–442 (2004).
44. Diaz, R. J. & Rosenberg, R. Marine benthic hypoxia: a review of its ecological effects and the behavioural responses of benthic macrofauna. *Oceanography and marine biology. An annual review* **33**, 03 (1995).
45. Keeling, R. F., Körtzinger, A. & Gruber, N. Ocean deoxygenation in a warming world. *Ann Rev Mar Sci* **2**, 199–229 (2010).
46. Breitburg, D. *et al.* Declining oxygen in the global ocean and coastal waters. *Science* (1979) **359**, (2018).
47. Zhao, P. *et al.* Metabolomic and proteomic responses of *Phaeodactylum tricornutum* to hypoxia. *J Oceanol Limnol* **40**, 1963–1973 (2022).

48. Wu, R. S. S., Wo, K. T. & Chiu, J. M. Y. Effects of hypoxia on growth of the diatom *Skeletonema costatum*. *J Exp Mar Biol Ecol* **420–421**, 65–68 (2012).
49. Roberts, K., Granum, E., Leegood, R. C. & Raven, J. A. Carbon acquisition by diatoms. *Photosynth Res* **93**, 79–88 (2007).
50. Yool, A. & Tyrrell, T. Role of diatoms in regulating the ocean's silicon cycle. *Global Biogeochem Cycles* **17**, (2003).
51. Zhao, D. *et al.* Disproportionate responses between free-living and particle-attached bacteria during the transition to oxygen-deficient zones in the Bohai Seawater. *Science of The Total Environment* **791**, 148097 (2021).
52. Mahmud, M. A. P. *et al.* Recent progress in sensing nitrate, nitrite, phosphate, and ammonium in aquatic environment. *Chemosphere* **259**, 127492 (2020).
53. Mills, G. & Fones, G. A review of *in situ* methods and sensors for monitoring the marine environment. *Sensor Review* **32**, 17–28 (2012).
54. Mohseni, F. *et al.* Ocean water quality monitoring using remote sensing techniques: A review. *Mar Environ Res* **180**, 105701 (2022).
55. Fascista, A. Toward integrated large-scale environmental monitoring using WSN/UAV/Crowdsensing: A review of applications, signal processing, and future perspectives. *Sensors* **22**, 1824 (2022).
56. Magliaro, C. *et al.* Oxygen consumption characteristics in 3D constructs depend on cell density. *Front Bioeng Biotechnol* **7**, (2019).
57. Chua, S. T. *et al.* Light management by algal aggregates in living photosynthetic hydrogels. *Proceedings of the National Academy of Sciences* **121**, (2024).
58. Willert, C. E. & Gharib, M. Digital particle image velocimetry. *Exp Fluids* **10**, 181–193 (1991).
59. Pacherres, C. O., Ahmerkamp, S., Koren, K., Richter, C. & Holtappels, M. Ciliary flows in corals ventilate target areas of high photosynthetic oxygen production. *Current Biology* **32**, 4150–4158.e3 (2022).
60. Bhatia, S. N. & Ingber, D. E. Microfluidic organs-on-chips. *Nat Biotechnol* **32**, 760–772 (2014).
61. Alique, M. *et al.* Hypoxia-inducible factor-1 α : The master regulator of endothelial cell senescence in vascular aging. *Cells* **9**, 195 (2020).
62. Gao, H. *et al.* Role of hypoxia in cellular senescence. *Pharmacol Res* **194**, 106841 (2023).
63. Chandel, N. S. & Budinger, G. R. S. The cellular basis for diverse responses to oxygen. *Free Radic Biol Med* **42**, 165–174 (2007).
64. Tao, J. *et al.* Targeting hypoxic tumor microenvironment in pancreatic cancer. *J Hematol Oncol* **14**, 14 (2021).
65. Singhal, R. & Shah, Y. M. Oxygen battle in the gut: Hypoxia and hypoxia-inducible factors in metabolic and inflammatory responses in the intestine. *Journal of Biological Chemistry* **295**, 10493–10505 (2020).

66. Nelson, J. A. Oxygen consumption rate v. rate of energy utilization of fishes: a comparison and brief history of the two measurements. *J Fish Biol* **88**, 10–25 (2016).
67. Astrup, A. & Tremblay, A. Energy metabolism. *Introduction to human nutrition* **31**, 48 (2009).
68. Müller, M. E. *et al.* Mitochondrial toxicity of selected micropollutants, their mixtures, and surface water samples measured by the oxygen consumption rate in cells. *Environ Toxicol Chem* **38**, 1000–1011 (2019).
69. Wallace, K. B. & Starkov, A. A. Mitochondrial targets of drug toxicity. *Annu Rev Pharmacol Toxicol* **40**, 353–388 (2000).
70. Bartlett, D. W. *et al.* The strobilurin fungicides. *Pest Manag Sci* **58**, 649–662 (2002).
71. Droppa, M., Horváth, G., Vass, I. & Demeter, S. Mode of action of Photosystem II herbicides studied by thermoluminescence. *Biochimica et Biophysica Acta (BBA) - Bioenergetics* **638**, 210–216 (1981).
72. Lee, S., Lee, H. & Kim, K.-T. Optimization of experimental conditions and measurement of oxygen consumption rate (OCR) in zebrafish embryos exposed to organophosphate flame retardants (OPFRs). *Ecotoxicol Environ Saf* **182**, 109377 (2019).
73. Preez, G. Du *et al.* Oxygen consumption rate of *Caenorhabditis elegans* as a high-throughput endpoint of toxicity testing using the Seahorse XFe96 Extracellular Flux Analyzer. *Sci Rep* **10**, 4239 (2020).
74. Attene-Ramos, M. S. *et al.* Systematic study of mitochondrial toxicity of environmental chemicals using quantitative high throughput screening. *Chem Res Toxicol* **26**, 1323–1332 (2013).
75. Espinosa, J. A., Pohan, G., Arkin, M. R. & Markossian, S. Real-time assessment of mitochondrial toxicity in HepG2 cells using the seahorse extracellular flux analyzer. *Curr Protoc* **1**, (2021).
76. Kim, C.-W., Lee, H.-J., Ahn, D., Go, R.-E. & Choi, K.-C. Establishment of a platform for measuring mitochondrial oxygen consumption rate for cardiac mitochondrial toxicity. *Toxicol Res* **38**, 511–522 (2022).
77. Costa, T., Vieira, R. F., Bizzo, H. R., Silveira, D. & Gimenes, M. A. Secondary metabolites. in (In: DHANARASU, S.(Ed.). *Chromatography and its applications*. Rijeka: InTech ..., 2012).
78. Croteau, R., Kutchan, T. M. & Lewis, N. G. Natural products (secondary metabolites). *Biochemistry and molecular biology of plants* **24**, 1250–1319 (2000).
79. Dow, L. *et al.* The multifaceted inhibitory effects of an Alkylquinolone on the diatom *Phaeodactylum tricorutum*. *ChemBioChem* **21**, 1206–1216 (2020).
80. Swift, S. *et al.* Quorum sensing as a population-density-dependent determinant of bacterial physiology. in 199–270 (2001). doi:10.1016/S0065-2911(01)45005-3.

81. Whalen, K. E. *et al.* Bacterial alkylquinolone signaling contributes to structuring microbial communities in the ocean. *Microbiome* **7**, 93 (2019).
82. Di Costanzo, F., Di Dato, V. & Romano, G. Diatom–bacteria interactions in the marine environment: Complexity, heterogeneity, and potential for biotechnological applications. *Microorganisms* **11**, 2967 (2023).
83. Zhang, Y. Cell toxicity mechanism and biomarker. *Clin Transl Med* **7**, (2018).
84. Andrew, A. S. *et al.* Genomic and proteomic profiling of responses to toxic metals in human lung cells. *Environ Health Perspect* **111**, 825–835 (2003).
85. Aslantürk, Ö. S. In vitro cytotoxicity and cell viability assays: principles, advantages, and disadvantages. *Genotoxicity-A predictable risk to our actual world* **2**, 64–80 (2018).
86. Frankfurt, O. S. & Krishan, A. Apoptosis-based drug screening and detection of selective toxicity to cancer cells. *Anticancer Drugs* **14**, 555–561 (2003).
87. Martins, G. The metabolic theory of ecology as a mechanistic approach. in 29–60 (2024). doi:10.1007/978-3-031-46917-6_3.
88. West, G. B. & Brown, J. H. The origin of allometric scaling laws in biology from genomes to ecosystems: towards a quantitative unifying theory of biological structure and organization. *Journal of Experimental Biology* **208**, 1575–1592 (2005).
89. Schramski, J. R., Dell, A. I., Grady, J. M., Sibly, R. M. & Brown, J. H. Metabolic theory predicts whole-ecosystem properties. *Proc Natl Acad Sci U S A* **112**, 2617–2622 (2015).
90. Heusner, A. A. Energy metabolism and body size I. Is the 0.75 mass exponent of Kleiber’s equation a statistical artifact? *Respir Physiol* **48**, 1–12 (1982).
91. Norin, T. & Gamperl, A. K. Metabolic scaling of individuals vs. populations: Evidence for variation in scaling exponents at different hierarchical levels. *Funct Ecol* **32**, 379–388 (2018).
92. Zaoli, S. *et al.* Generalized size scaling of metabolic rates based on single-cell measurements with freshwater phytoplankton. *Proc Natl Acad Sci U S A* **116**, 17323–17329 (2019).
93. Dixit, C. K. & Kaushik, A. *Microfluidics for Biologists: Fundamentals and Applications*. *Microfluidics for Biologists: Fundamentals and Applications* (Springer International Publishing, 2016). doi:10.1007/978-3-319-40036-5.
94. Niculescu, A. G., Chircov, C., Bîrcă, A. C. & Grumezescu, A. M. Fabrication and applications of microfluidic devices: A review. *International Journal of Molecular Sciences* vol. 22 1–26 Preprint at <https://doi.org/10.3390/ijms22042011> (2021).

95. Riahi, R. *et al.* Microfluidics for advanced drug delivery systems. *Curr Opin Chem Eng* **7**, 101–112 (2015).
96. Lee, W. G., Kim, Y.-G., Chung, B. G., Demirci, U. & Khademhosseini, A. Nano/Microfluidics for diagnosis of infectious diseases in developing countries. *Adv Drug Deliv Rev* **62**, 449–457 (2010).
97. Jahn, A. *et al.* Preparation of nanoparticles by continuous-flow microfluidics. *Journal of Nanoparticle Research* **10**, 925–934 (2008).
98. Miyajima, H. & Mehregany, M. High-aspect-ratio photolithography for MEMS applications. *Journal of Microelectromechanical Systems* **4**, 220–229 (1995).
99. Qin, D., Xia, Y. & Whitesides, G. M. Soft lithography for micro- and nanoscale patterning. *Nat Protoc* **5**, 491–502 (2010).
100. Iliescu, C., Tan, K. L., Tay, F. E. H. & Miao, J. Deep wet and dry etching of Pyrex glass: A review. in *Proceedings of the ICMAT (Symposium F), Singapore 75–78* (Citeseer, 2005).
101. Ho, C. M. B., Ng, S. H., Li, K. H. H. & Yoon, Y.-J. 3D printed microfluidics for biological applications. *Lab Chip* **15**, 3627–3637 (2015).
102. Au, A. K., Huynh, W., Horowitz, L. F. & Folch, A. 3D-printed microfluidics. *Angewandte Chemie International Edition* **55**, 3862–3881 (2016).
103. Nielsen, A. V., Beauchamp, M. J., Nordin, G. P. & Woolley, A. T. 3D printed microfluidics. *Annual Review of Analytical Chemistry* **13**, 45–65 (2020).
104. Mata, A., Fleischman, A. J. & Roy, S. Characterization of polydimethylsiloxane (PDMS) properties for biomedical micro/nanosystems. *Biomed Microdevices* **7**, 281–293 (2005).
105. McDonald, J. C. *et al.* Fabrication of microfluidic systems in poly(dimethylsiloxane). *Electrophoresis* **21**, 27–40 (2000).
106. Iliescu, C., Taylor, H., Avram, M., Miao, J. & Franssila, S. A practical guide for the fabrication of microfluidic devices using glass and silicon. *Biomicrofluidics* **6**, (2012).
107. Li, X., Abe, T. & Esashi, M. Deep reactive ion etching of Pyrex glass using SF₆ plasma. *Sens Actuators A Phys* **87**, 139–145 (2001).
108. Spierings, G. A. C. M. Wet chemical etching of silicate glasses in hydrofluoric acid based solutions. *J Mater Sci* **28**, 6261–6273 (1993).
109. Iliescu, C., Tay, F. E. H. & Miao, J. Strategies in deep wet etching of Pyrex glass. *Sens Actuators A Phys* **133**, 395–400 (2007).
110. Manz, A., Graber, N. & Widmer, H. M. Miniaturized total chemical analysis systems: A novel concept for chemical sensing. *Sens Actuators B Chem* **1**, 244–248 (1990).
111. Francesko, A., Cardoso, V. F. & Lanceros-Méndez, S. Lab-on-a-chip technology and microfluidics. in *Microfluidics for Pharmaceutical Applications* 3–36 (Elsevier, 2019). doi:10.1016/B978-0-12-812659-2.00001-6.

112. Kuru, C. İ., Ulucan-Karnak, F. & Akgöl, S. Lab-on-a-chip sensors. in *Fundamentals of Sensor Technology* 65–98 (Elsevier, 2023). doi:10.1016/B978-0-323-88431-0.00012-0.
113. Azimzadeh, M. *et al.* Microfluidic-based oxygen (O₂) sensors for on-chip monitoring of cell, tissue and organ metabolism. *Biosensors (Basel)* **12**, 6 (2021).
114. Liebisch, F., Weltin, A., Marzioch, J., Urban, G. A. & Kieninger, J. Zero-consumption Clark-type microsensor for oxygen monitoring in cell culture and organ-on-chip systems. *Sens Actuators B Chem* **322**, 128652 (2020).
115. Luo, J., Dziubla, T. & Eitel, R. A low temperature co-fired ceramic based microfluidic Clark-type oxygen sensor for real-time oxygen sensing. *Sens Actuators B Chem* **240**, 392–397 (2017).
116. Morris, M. J. *et al.* Aerodynamic applications of pressure sensitive paint. *AIAA Journal* **31**, 419–425 (1993).
117. McDonagh, C., Burke, C. S. & MacCraith, B. D. Optical chemical sensors. *Chem Rev* **108**, 400–422 (2008).
118. Koren, K., Brodersen, K. E., Jakobsen, S. L. & Köhl, M. Optical sensor nanoparticles in artificial sediments—a new tool to visualize O₂ dynamics around the rhizome and roots of seagrasses. *Environ Sci Technol* **49**, 2286–2292 (2015).
119. Amao, Y., Miyashita, T. & Okura, I. Platinum tetrakis(pentafluorophenyl)porphyrin immobilized in polytrifluoroethylmethacrylate film as a photostable optical oxygen detection material. *J Fluor Chem* **107**, 101–106 (2001).
120. Mateen, F. *et al.* Polymer dispersed liquid crystal device with integrated luminescent solar concentrator. *Liq Cryst* **45**, 498–506 (2018).
121. Lee, S.-K. & Okura, I. Photostable Optical Oxygen Sensing Material: Platinum Tetrakis(pentafluorophenyl)porphyrin Immobilized in Polystyrene. *Analytical Communications* **34**, 185–188 (1997).
122. Mistlberger, G. *et al.* Multifunctional magnetic optical sensor particles with tunable sizes for monitoring metabolic parameters and as a basis for nanotherapeutics. *Adv Funct Mater* **20**, 1842–1851 (2010).
123. Koren, K., Jakobsen, S. L. & Köhl, M. In-vivo imaging of O₂ dynamics on coral surfaces spray-painted with sensor nanoparticles. *Sens Actuators B Chem* **237**, 1095–1101 (2016).
124. Yoshihara, T., Hirakawa, Y., Hosaka, M., Nangaku, M. & Tobita, S. Oxygen imaging of living cells and tissues using luminescent molecular probes. *Journal of Photochemistry and Photobiology C: Photochemistry Reviews* **30**, 71–95 (2017).
125. Zhdanov, A. V., Golubeva, A. V., Okkelman, I. A., Cryan, J. F. & Papkovsky, D. B. Imaging of oxygen gradients in giant umbrella cells: an ex vivo PLIM study. *American Journal of Physiology-Cell Physiology* **309**, C501–C509 (2015).

126. Okkelman, I. A., Neto, N., Papkovsky, D. B., Monaghan, M. G. & Dmitriev, R. I. A deeper understanding of intestinal organoid metabolism revealed by combining fluorescence lifetime imaging microscopy (FLIM) and extracellular flux analyses. *Redox Biol* **30**, 101420 (2020).
127. Ehgartner, J. *et al.* Online analysis of oxygen inside silicon-glass microreactors with integrated optical sensors. *Sens Actuators B Chem* **228**, 748–757 (2016).
128. Ungerböck, B., Charwat, V., Ertl, P. & Mayr, T. Microfluidic oxygen imaging using integrated optical sensor layers and a color camera. *Lab Chip* **13**, 1593 (2013).
129. Stockdale, A., Davison, W. & Zhang, H. Micro-scale biogeochemical heterogeneity in sediments: a review of available technology and observed evidence. *Earth Sci Rev* **92**, 81–97 (2009).
130. Frederiksen, M. S. & Glud, R. N. Oxygen dynamics in the rhizosphere of *Zostera marina*: A two-dimensional planar optode study. *Limnol Oceanogr* **51**, 1072–1083 (2006).
131. Meysman, F. J. R., Galaktionov, O. S., Glud, R. N. & Middelburg, J. J. Oxygen penetration around burrows and roots in aquatic sediments. (2010).
132. Larsen, M., Santner, J., Oburger, E., Wenzel, W. W. & Glud, R. N. O₂ dynamics in the rhizosphere of young rice plants (*Oryza sativa* L.) as studied by planar optodes. *Plant Soil* **390**, 279–292 (2015).
133. Holst, G. A., Franke, U. & Grunwald, B. Transparent oxygen optodes in environmental applications at fine scale as measured by luminescence lifetime imaging. in *Advanced Environmental Sensing Technology II* vol. 4576 138–148 (SPIE, 2002).
134. Koren, K., Jakobsen, S. L. & Köhl, M. In-vivo imaging of O₂ dynamics on coral surfaces spray-painted with sensor nanoparticles. *Sens Actuators B Chem* **237**, 1095–1101 (2016).
135. Schindelin, J. *et al.* Fiji: an open-source platform for biological-image analysis. *Nat Methods* **9**, 676–682 (2012).
136. Chem ; Beckett, C. W., Pitzer, K. S., Spitzer, R. & Amer, J. *Determination of Dry Mass, Thickness, Solid and Water Concentration in Living Cells*. *Bergv. Met* vol. 32 (1936).
137. Barer, R. Determination of dry mass, thickness, solid and water concentration in living cells. *Nature* **172**, 1097–1098 (1953).
138. Nguyen, T. L. *et al.* Quantitative phase imaging: recent advances and expanding potential in biomedicine. *ACS Nano* **16**, 11516–11544 (2022).
139. Barer, R. & Joseph, S. Refractometry of living cells part I. Basic principles. *J Cell Sci* **3**, 399–423 (1954).
140. Arzumanyan, V. A., Kiseleva, O. I. & Poverennaya, E. V. The Curious Case of the HepG2 Cell Line: 40 Years of Expertise. *Int J Mol Sci* **22**, 13135 (2021).

141. Falciatore, A., Jaubert, M., Bouly, J.-P., Bailleul, B. & Mock, T. Diatom molecular research comes of age: Model species for studying phytoplankton biology and diversity. *Plant Cell* **32**, 547–572 (2020).
142. Yang, C. *et al.* Morphological and physicochemical characteristics, biological functions, and biomedical applications of diatom frustule. *Algal Res* **72**, 103104 (2023).
143. Wu, R. S. S. Hypoxia: from molecular responses to ecosystem responses. *Mar Pollut Bull* **45**, 35–45 (2002).
144. Sun, J.-Z. *et al.* Enhancement of diatom growth and phytoplankton productivity with reduced O₂ availability is moderated by rising CO₂. *Commun Biol* **5**, 54 (2022).
145. Botte, E. *et al.* Scaling of joint mass and metabolism fluctuations in in silico cell-laden spheroids. *Proceedings of the National Academy of Sciences* **118**, (2021).

Acta Universitatis Upsaliensis

Digital Comprehensive Summaries of Uppsala Dissertations from the Faculty of Science and Technology 2424

Editor: The Dean of the Faculty of Science and Technology

A doctoral dissertation from the Faculty of Science and Technology, Uppsala University, is usually a summary of a number of papers. A few copies of the complete dissertation are kept at major Swedish research libraries, while the summary alone is distributed internationally through the series Digital Comprehensive Summaries of Uppsala Dissertations from the Faculty of Science and Technology. (Prior to January, 2005, the series was published under the title “Comprehensive Summaries of Uppsala Dissertations from the Faculty of Science and Technology”.)

Distribution: publications.uu.se
urn:nbn:se:uu:diva-535367



ACTA UNIVERSITATIS
UPSALIENSIS
2024